Research Report 2022
Volume 34

In this volume…

Report Summaries

For ***Complete Reports*** *and* ***Student Theses*** *please visit:*

https://www.crewes.org

(Sign in/password required)

UNIVERSITY OF CALGARY
FACULTY OF SCIENCE
Department of Geoscience

Notice of Intent to Publish

Please note that the authors of the research in this 34th Volume of the Abstract Book intend to publish or otherwise publically disseminate their full research papers in the coming calendar year. According to the contracts between the University of Calgary (CREWES) and each Sponsor, the University will make available to the Sponsor a copy of the proposed publication resulting from the CREWES Project prior to submission for publication. In the event that the Sponsor determines that Research Results within the proposed publication contain Sponsor Confidential Information, the Sponsor shall have thirty (30) days to notify the University in writing and the University shall remove Sponsor Confidential information prior to publication. This 30 day period shall be considered to have started at the end of this meeting (December 2, 2022). These full research reports are available on the CREWES website to all Sponsors and their employees.

CREWES in 2022

Once again in 2022 I have the honour and pleasure of welcoming you to the CREWES Annual Sponsor's Meeting and technical review. As you can see from this collection of abstracts, we have been hunting big scientific game again in 2022. I'm delighted you'll be able to see the high impact and wide ranging results the students, staff, and researchers in CREWES have produced this year.

Of course, the big news item is that we are back in person! We have missed having the in-person feel of the meeting, the beautiful scenic backdrop of Banff, and the opportunities for interactions that are difficult to achieve in an online format. That said, the online format allowed larger numbers of sponsor reps from each partner and collaborating organization to join. And potentially had a larger reach and impact. With that in mind, we are trying out a hybrid experience this year. Including an in-person Banff meeting that is streamed to remote participants, and also recorded for later viewing. It is a field experiment just like so much of our research – we'll be interested in feedback on how it went, how accessible it made the science, and whether we should repeat it again next year.

From a technical point of view, the relaxation of many of the COVID restrictions and protocols in Canada in 2022 allowed some long-planned field research to take place. This year we carried out a number of customized field experiments which have produced a set of globally unique datasets. First, we returned to the Containment and Monitoring Institute's Newell County Facility for a repeat of the multi-azimuth and multi-offset DAS and broadband VSP we acquired in 2018. This time with partners Echo Seismic and HDVSP. This not only updates our side by side sensor comparison datasets, but it adds a time lapse element to our CO2 monitoring initiatives. Expect to hear a lot about the "Snowflake Time Lapse" data in the coming years. We also returned to the field to build up on our rapid repeat fixed source experiments, which are producing fascinating new science – we will be reporting on that this week in a number of talks.

This year also sees a major expansion of our FWI work on field and ultrasound data, our work on proper parameterization of elastic FWI for rock-physics and other reservoir applications, our efforts in carrying out seismic processing in the context of machine learning tools and architectures, and next generation ideas for geophysics, with quantum tools, and geothermal and CO2 applications, all in development.

CREWES relies completely on the financial support of our sponsors. For this support we are extremely grateful. It is our goal is to repay the effort with big, high impact results. We look forward to working with our partners and colleagues in 2023 and beyond!

Calgary, Alberta	Kris Innanen
November, 2022	CREWES Director

Table of Contents

---

* Presenter

2022 CREWES Sponsors

Acceleware	Aramco Services Company
CGG	Chevron Corporation
CNPC-RIPED	Devon Energy Corporation
INOVA Geophysical	Japan Oil, Gas and Metals National Corporation
Petrobras	
TGS	Petronas Carigali SDN BHD

Natural Sciences and Engineering Research Council of Canada (NSERC) - Collaborative Research and Development Grant

NSERC
CRSNG

Additional funding provided by:

CANADA FIRST
RESEARCH EXCELLENCE FUND

CREWES Personnel 2022

LEADERSHIP

Kristopher A. Innanen, Director
Professor, Department of Geoscience, University of Calgary

B.Sc. Physics and Earth Science, 1996, York University
M.Sc. Physics, 1998, York University
Ph.D. Geophysics, 2003, University of British Columbia

- Work Experience: University of Houston

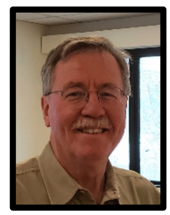

Don C. Lawton, Associate Director
Director for Containment and Monitoring Institute (CaMI)

Faculty Professor, Department of Geoscience, University of Calgary

B.Sc. (Hons. Class I) Geology, 1973, University of Auckland
Ph.D. Geophysics, 1979, University of Auckland

- Work Experience: New Zealand Steel Mining Ltd., Amoco Minerals (N.Z.) Ltd., Carbon Management Canada

Daniel Trad, Associate Director
Associate Professor, Department of Geoscience, University of Calgary

Licenciatura in Geophysics, 1994, Universidad Nacional de San Juan, Argentina
Ph.D Geophysics, 2001, University of British Columbia

- Work Experience: Electromagnetic Methods (Argentina and Brazil), Seismic Research and development (Veritas, CGG, Techco, in Calgary and France)

Kevin W. Hall, Technical Manager

B.Sc. Geophysics, 1992, University of Calgary
M.Sc. Geophysics, 1996, University of Calgary

- Work Experience: Lithoprobe Seismic Processing Facility at the University of Calgary

RESEARCH STAFF, POST DOCS AND VISITING SCHOLARS

Kevin L. Bertram

Electronics Technician Certificate, 2005, Southern Alberta Institute of Technology

- Work Experience: Aram Systems Ltd.

Malcolm B. Bertram

B.Sc. Geology, Auckland, New Zealand

- Work Experience: GSI (Western Australia), Western Geophysics (Western Australia), Auckland University, University of Calgary

Xiaohui Cai

B.Sc. Geophysics, 2011, Yangtze University, Hubei, China
Ph.D. Geophysics, 2016, China University of Petroleum

- Work Experience: Nanjing Tech University, The University of Texas at Austin

Marcelo Guarido de Andrade

B.Sc. Physics, 2006, University of São Paulo, Brazil
M.Sc. Geophysics, 2008, University of São Paulo, Brazil
Ph.D. Geophysics, 2017, University of Calgary

- Work Experience: Verdazo Analytics, Schlumberger (Houston), PGS (Rio de Janeiro, Brazil), Orthogonal Geophysics, Husky Energy

David C. Henley

B.Sc. Physics, 1967, Colorado State University
M.Sc. Physics, 1968, University of Michigan

- Work Experience: Shell Oil Co., Shell Canada Ltd.

Helen Isaac

B.Sc. Mathematics, 1973, Imperial College, London
M.Sc. Geophysics, 1974, Imperial College, London
Ph.D. Geophysics, 1996, University of Calgary

- Work Experience: Phillips Petroleum Company, Hudson's Bay Oil and Gas, Canterra Energy, Husky, Fold-Fault Research Project at the University of Calgary

Scott Keating

B.Sc. with Honours in Physics 2014, University of Alberta
Ph.D. Geophysics, 2020, University of Calgary

- Work Experience: CNOOC International

Jing Wang

B.Sc. Geophysics, 2016, Northeast Petroleum University
M.Sc. Geological Resources and Geological Engineering, 2018, China University of Petroleum (Beijing)

Yichuan Wang

B.Sc. Geological Engineering, 2013, China University of Mining and Technology, Beijing, China
Ph.D. Geophysics, 2019, University of Saskatchewan

- Work Experience: Joanneum Research, The University of Oklahoma

Joe Wong

B.Sc. Physics/Mathematics, 1971, Queen's University
M.Sc. Applied Geophysics, 1973, University of Toronto
Ph.D. Applied Geophysics, 1979, University of Toronto
Work Experience: Ontario Ministry of the Environment, University of Toronto, JODEX Applied Geoscience Limited, CREWES

GRADUATE STUDENTS

Ninoska Amundaray

B.Sc. Geophysical Engineering, 2016, Simon Bolivar University, Venezuela

- Work experience: PDVSA, Chevron Canada

Chioma Chineke

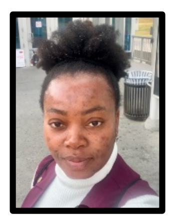

B.Sc. Applied geophysics 2010, Obafemi Awolowo University, Nigeria
MSc Geophysics 2016, University of Lagos, Nigeria

- Work experience: Degeconek Nigeria limited

David J.Emery

M.Sc. Geophysics, 2006, University of Calgary

- Work experience: Husky Energy

Paloma Lira Fontes

B.Sc. Geophysics, 2018, Federal University of Bahia

- Work experience: Canacol Energy Ltd.

Xin Fu

B.Sc. Geophysics, 2015, China University of Petroleum (East China)

M.Sc. Geophysics, 2018, China University of Petroleum(Beijing)

Scott Hess

B.Sc. Geophysical Engineering, 2003, Montana Technological University

M.Sc. Geophysics, 2006, Boise State University

- Work Experience: Equinor

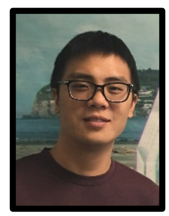

Qi Hu

B.Sc. Geophysics, 2011, Yangtze University, Hubei, China

M.Sc. Geophysics, 2014, China University of Petroleum, China

- Work Experience: Sinopec Geophysical Research Institute

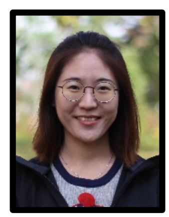

Shang Huang

B.Eng. Geophysics, 2017, China University of Petroleum, China

M.Sc. Geophysics, 2018, University of Calgary

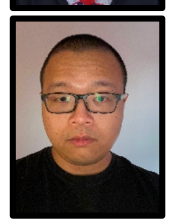

Ji Li

B.Sc. with Honours in Geophysics 2018, University of Alberta

M.Sc. Geophysics, 2021, University of Alberta

Jinji Li

B.Sc. Exploration Geophysics, 2017, Ocean University of China

M.Sc. Geophysics, 2020, Tongji University

- Work Experience: The First Institute of Oceanography of China, DTCC

He Liu

B.Sc. Prospecting Technology and Engineering, 2012, China University of Petroleum (Beijing)
M.Sc. Geophysics, 2014, China University of Petroleum (Beijing)
Ph.D. Geophysics, 2019, China University of Petroleum (Beijing)

Mariana Lume

B.Sc. Geophysical Engineering, 2019, Simon Bolivar University
- Work Experience: PDVSA Intevep, TAQA North

Jorge Monsegny

B.Sc. Computer Science, 2003, National University of Colombia
M.Sc. Mathematics, 2007, National University of Colombia
- Work Experience: Santander Industrial University, Ecopetrol ICP, National University of Colombia

Kimberly Pike

B.Sc. with Honours in Earth Sciences, 2001, University of Newfoundland
M.Sc. Geophysics, 2014, University of Calgary
- Work Experience: Strategic Oil & Gas, Obsidian Energy, Enerplus Corporation, Devon Energy, EnCana Corporation

Luping Qu

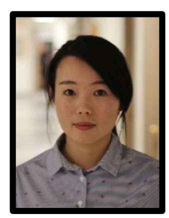

B.Sc. Geophysics, 2014, China University of Petroleum (East China)
M.Sc. Geophysics, 2017, China University of Petroleum (Beijing)

Sarah Reid

B.Sc. with honours Geophysics, 2019, University of Calgary
- Work Experience: ARC Resources

Lukas Sadownyk

B.Sc. with honours Geophysics, 2020, University of Calgary
B.Sc. with distinction Geology, 2020, University of Calgary

- Work Experience: Valeura Energy, Gran Tierra, Imperial Oil, CNRL

Ziguang Su

B.Eng. Exploration Geophysics, 2017, China University of Petroleum, China
B.A. English, 2017, China University of Petroleum
M.Sc. Geophysics, 2018, University of Calgary

Tianze Zhang

B.Sc. Applied Geophysics, 2015, Jilin University, China
M.Sc. Geological Engineering, 2018, Jilin University, China

Kai Zhuang

B.Sc. Geophysics, 2018, University of Calgary

ASSOCIATED FACULTY and SCIENTISTS

Huaizhen Chen

Research Fellow, Tongji University, Shanghai, China
Adjunct Researcher, CREWES, University of Calgary

Ph.D. Geophysics, 2015, China University of Petroleum
B.Sc. Geophysics, 2010, China University of Petroleum

Andreas Cordsen

Technical Advisor, CREWES, University of Calgary

M.Sc. Geology, 1975, Queen's University, Kingston
M.Sc. Geophysics, 1980, Dalhousie University, Halifax

- Work Experience: BEB, Esso Resources, Norcen Energy, GEDCO, Schlumberger, CHAD Data Ltd.

Sam Gray

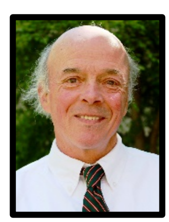

Technical Advisor, CREWES, University of Calgary

B.S. Math, 1970, Georgetown University
Ph.D. Math, 1978, University of Denver

- Work experience: U.S. Naval Research Lab, General Motors Institute, Amoco, BP, Veritas, CGG

Rachel Lauer
Assistant Professor, University of Calgary

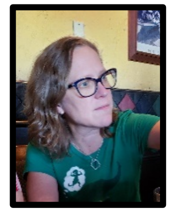

B.Sc. Psychology, Bryn Mawr College
M.Sc. Environmental Engineering Geoscience, Radford University
Ph.D. Geoscience, Pennsylvania State University

- Work Experience: Consultant at NAEVA Geophysics

Faranak Mahmoudian
Technical Advisor, CREWES, University of Calgary

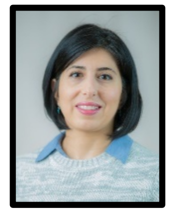

B.Sc. Applied Physics, 2000, K. N. Toosi University of Technology, Iran
M.Sc. Geophysics, 2006, University of Calgary
Ph.D. Geophysics, 2013, University of Calgary

- Work Experience: Shell Canada, Earth Signal Processing

Gary F. Margrave, Emeritus Director
Emeritus Professor, Faculty Professor, Department of Geoscience, University of Calgary

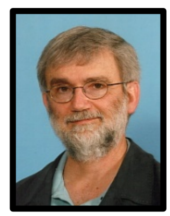

B.Sc. Physics, 1975, University of Utah
M.Sc. Physics, 1977, University of Utah
Ph.D. Geophysics, 1981, University of Alberta

- Work Experience: Chevron Canada Resources, Chevron Geoscience Company, Devon Canada, TGS Canada

Brian H. Russell
Adjunct Professor, Department of Geoscience, University of Calgary

B.Sc. Physics, 1972, University of Saskatchewan
Honours Certificate in Geophysics, 1975, University of Saskatchewan
M.Sc. Geophysics, 1978, University of Durham
Ph.D. Geophysics, 2004, University of Calgary

- Work Experience: Chevron Geoscience Company, Teknica Resource Development, Veritas Software Ltd., Hampson-Russell Software Ltd, GeoSoftware

Roman Shor
Associate Professor and Energi Simulation Industrial Research Chair in Geothermal Systems, Department of Chemical and Petroleum Engineering, University of Calgary

B.Sc. Computer Science, 2009, University of Pennsylvania
M.Sc. Computer Science, 2010, University of Pennsylvania
M.Sc. Petroleum Engineering, 2014, University of Texas at Austin
Ph.D. Petroleum Engineering, 2016, University of Texas at Austin

- Work Experience: Shell, Merck, Lehman Brothers

Robert R. Stewart
Cullen Chair in Exploration Geophysics, University of Houston
Adjunct Professor, Department of Geoscience, University of Calgary

B.Sc. Physics and Mathematics, 1978, University of Toronto
Ph.D. Geophysics, 1983, Massachusetts Institute of Technology

- Work Experience: Veritas Software Ltd., Gennix Technology Corp., University of Calgary

Xiucheng Wei
Technical Advisor, CREWES, University of Calgary

B.Sc. Geophysics, 1982, China University of Petroleum
M.Sc. Geophysics, 1992, China University of Petroleum
Ph.D. Geophysics, 1995, China University of Petroleum

- Work Experience: China National Petroleum Company (CNPC), China University of Petroleum (CUP), British Geological Survey (BGS), China Petroleum & Chemical Corporation (Sinopec), International Research Coordinator with the Faculty of Science at the University of Calgary

Matt Yedlin
Associate Professor, Department of Electrical and Computer Engineering, University of British Columbia

B.Sc. Honours Physics, 1971, University of Alberta
M.Sc. Physiology, 1973, University of Toronto
Ph.D. Geophysics, 1978, University of British Columbia

- Work Experience: Conoco

Student Theses

The following theses were completed with CREWES in 2022:

Ph.D.	Matthew Vernon Eaid	Distributed acoustic sensing: modelling, full waveform inversion, and its use in seismic monitoring
M.Sc.	Brendan Kolkman-Quinn	Time-lapse VSP monitoring of CO_2 sequestration at the CaMI Field Research Station
Ph.D.	Bernard Ki-Yun Law	Traveltime tomography for land seismic data
M.Sc.	Lukas Sadownyk	Optimizing Diagnostic Fracture Injection Test (DFIT) interpretation using Machine Learning (ML) methods

Well-log parameterized full waveform inversion 1: analysis of the single parameter case

Ninoska Amundaray*, Scott Keating, Matthew Eaid, and Kris Innanen

ABSTRACT

Applications of multiparameter elastic full waveform inversion (EFWI) deal with several challenges posed by the intrinsic nonlinearity of technique. Parameter cross-talk is one of most critical examples of the latter. Though, existing resources like scattering radiation patterns and the addition of prior information into FWI formulations might provide means to prevent some level of cross-talk. Ultimately, they cannot guarantee the removal of these unwanted effects. As an alternative mitigation strategy, we are studying reducing the numbers of modeled parameters in an isotropic medium, from three to one in this study. We argue that the single parameter inversion can be constructed in any application where elastic parameters demonstrate a strong correlation in readily available data, like well-logs, by fitting a trendline. An example of strong parameter relationship was observed and formulated for the Carbon Management Canada Newell County Facility. Though, the single parameter formulation was previously analyzed. We are expanding its use in a synthetic time-lapse application for carbon dioxide (CO_2) sequestration at the same site. Current results demonstrate that inverted models converged towards the true solution with various levels of success. While inverted P-wave velocity (V_P) and S-wave velocity (V_S) values fluctuate between a small parameter overestimation and underestimation. Density (ρ) values are mostly overestimated.

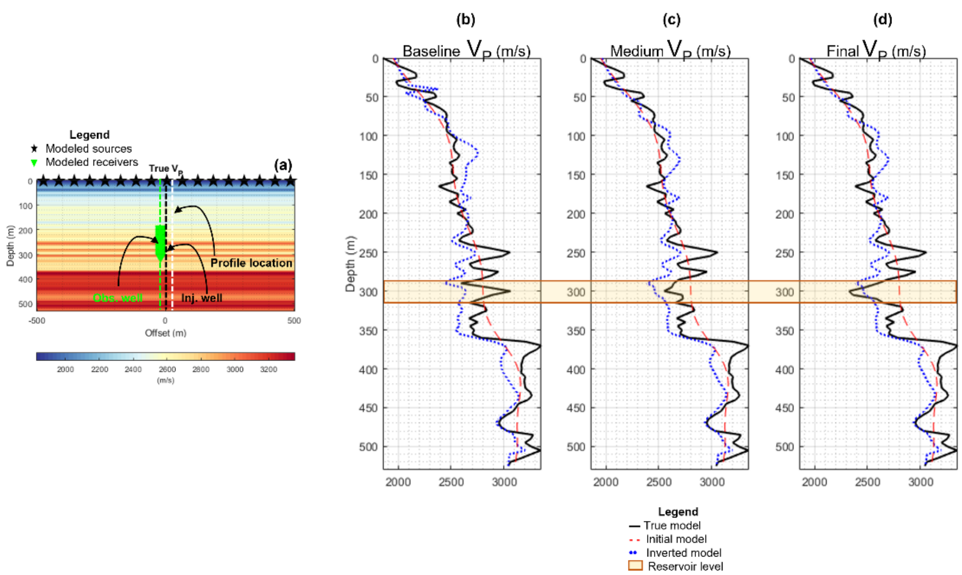

FIG. 1. (a) Shows an example of a velocity model used during in investigation overlaid by the simulated seismic acquisition, which has black stars indicating the modeled sources and green triangles indicating the receiver locations. V_P values for the profile location highlighted in (a) with a white dashed line is further detailed in (b) for a baseline stage, (c) for a medium stage of CO_2 injection, and (d) for a final stage of CO_2 injection. For these, the black lines indicate the true model, the red dashed lines indicate the initial model, the blue dotted lines are the inverted model, and the yellow box indicates the reservoir.

Well-log parameterized full waveform inversion 2: formulation of the two-parameter case

Ninoska Amundaray, Scott Keating, Matthew Eaid, and Kris Innanen

ABSTRACT

Addition of prior information in elastic full waveform inversion (EFWI) tends to aid faster and better model convergence by prioritizing relevant features of the medium where the simulated waveform is propagating. When this is employed as a parameterization, FWI formulations can be slightly simplified by reducing the number of terms used during the inversion. This idea was previously applied to an isotropic-elastic medium, which utilized the correlation between well-log data to aid the construction of a single parameter by fitting a trendline. While, models obtained using a version of the single log-guided parameterization have demonstrated encouraging results when little data variation exists. In this study, we advocate the inclusion of another parameter to this type of formulation, as way to (1) capture larger data variation and (2) expand the applicability of the formulation. To accomplish this, we propose a method that captures information from a direction omitted by the first parameter (or trendline), by combining spatial geometry with principal component analysis (PCA). Current results obtained using the updated log-guided parameterization demonstrate some positive remarks in terms of model convergence and measured parameter variation. But, to further exploit the addition of the second term in FWI applications, more understanding about parameter tuning must be carry out.

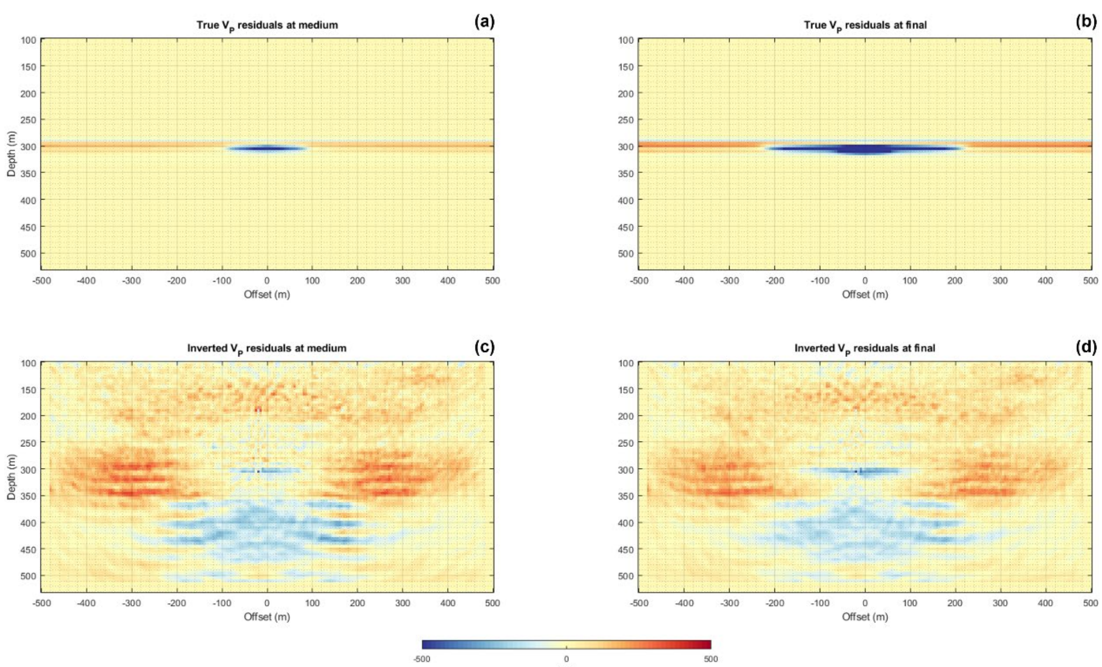

FIG. 1. Example of P-wave velocity residuals obtained in a time-lapse application using the two-parameter log-guided parameterization. Models in (a) and (b) are the true model residuals from two different stages, and models in (c) and (d) are the inverted model residuals.

Field school 2022, exposing the geoscientists of tomorrow to field acquisition methods

Kevin L. Bertram, Kris Innanen, Kevin W. Hall, Malcolm Bertram, Sarah Reid, and Wing Chan

ABSTRACT

This is the second in person field school since 2020. Although there was a field school last year, it was missing the reflections survey that had been traditionally carried out. This year saw the return of this. However, participation numbers are still lower than in years past and this year's field school was shorter than most. The University of Calgary's geophysics field school is often one of the first time that students have the opportunity to witness and operate the equipment used for collecting data that that have been, or will be, studying. This provides a vital link in the thought process as to why certain raw data may appear as it does. And it grants an understanding that data collection in the outside environment doesn't always conform to simulated data often used for teaching processing and interpolation methods. All acquisition was performed ath the Carbon Management Canada Newell County Facility (formerly the CaMI Field Research Station) near the town of Brooks, Alberta.

FIG. 1. Students learning about field data acquisition.

Recent upgrades to seismic physical modelling

Kevin L. Bertram* and Joe Wong

ABSTRACT

A new, more robust water tank with reinforced acrylic sides was built for the Seismic Physical Modelling Laboratory. The new tank replaces older versions that failed under prolonged water pressure. In addition, we performed measurements to characterize the wavelet shapes and 2D radiation patterns of three types of transducers operating in water. These were done to determine their effectiveness for producing low-frequency data suitable for efficient FWI. Furthermore, we designed and produced an Arbitrary Waveform Generator and evaluated its use for producing source-driving functions more complicated than simple impulses.

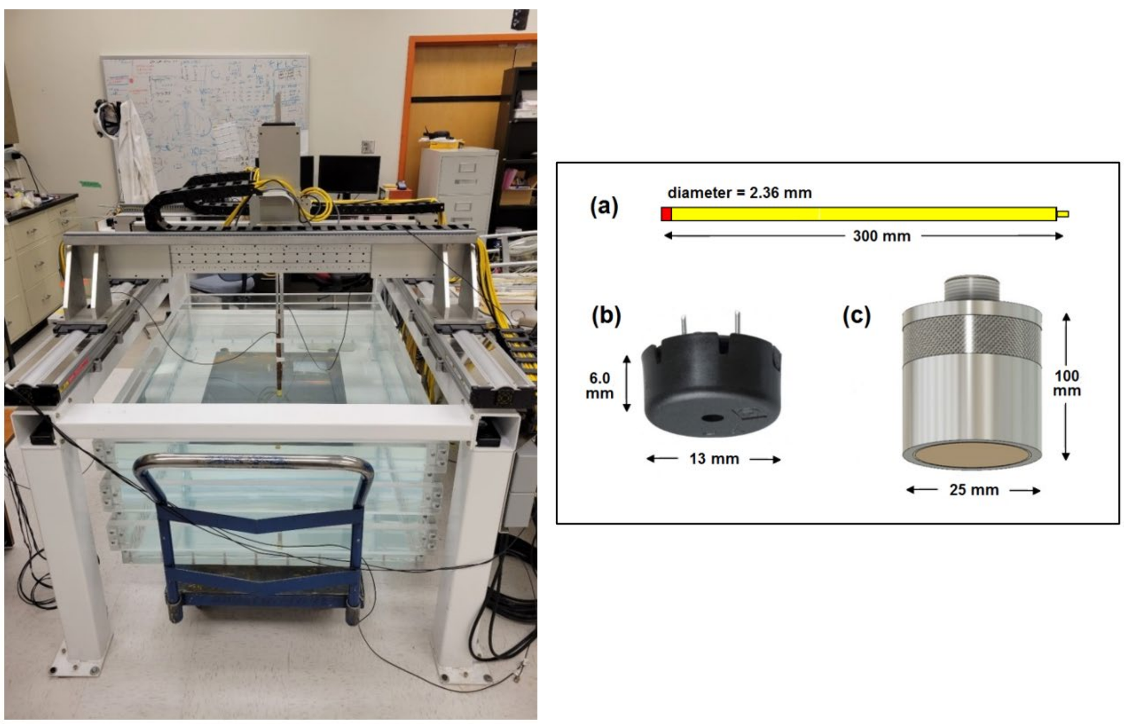

FIG. 1. Left: Photograph of the physical modeling setup, showing the new acrylic tank filled with water. Also shown are two Murata piezoelectric buzzers attached to the ends two small-diameter copper pipes and mounted on the physical modelling positioning subsystem. Right: Three types of transducers evaluated for producing low-frequency seismic data suitable for FWI. The dominant frequencies of source wavelets produced by the transducers are roughly inversely proportional to their diameters.

Analysis of the FWI workflow for accelerometer and DAS data from the 2018 CaMI VSP survey

Xiaohui Cai, Kris Innanen, Tianze Zhang, Kevin W. Hall, and Matt Eaid

ABSTRACT

In 2018, the Containment and Monitoring Institute Field Research Station (CaMI-FRS) in Newell County Alberta, which is part of CMC, carried out a 3D vertical seismic profile (VSP) (snowflake data) using three-component accelerometer and distributed acoustic sensing fibers (DAS). Eaid (2021a) have processed line 1 of the snowflake data to prepare them for inclusion in full waveform inversion. In this report, we mainly follow the processing and FWI workflow to inversion for the other line of the the snowflake data to detect the anisotropy of the area. Here, we use P-wave velocity parameterization frequency-domain FWI and effective source estimation schemes to implement the elastic properties inversion. The Figure 1 shows the inverted models of V_P, V_S, and ρ for the line 4 and line 1 of the snowflake data, where the line 1 have been processed by Eaid last year. From the Figure 1, we can see that the anisotropy exists in the field data, but the anisotropy is not strong.

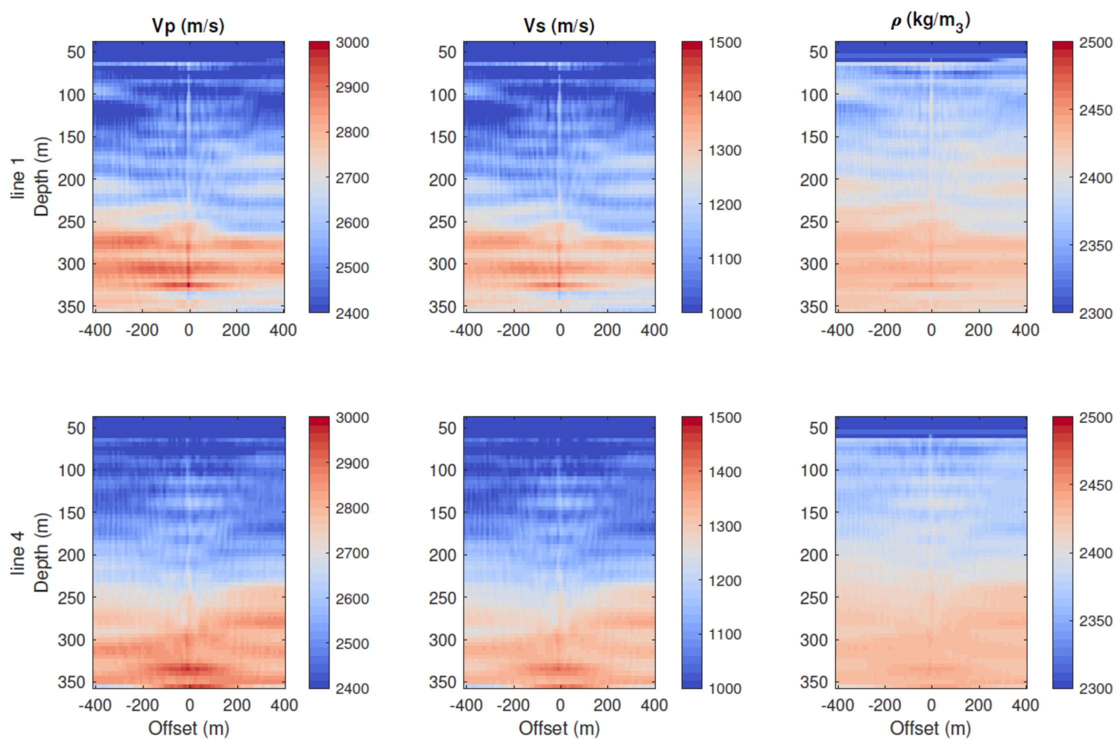

FIG. 1. Elastic FWI for the Line 1 and the Line 4 of the snowflake accelerometer and DAS data.

VSP imaging of CO_2 injection with rapid-repeat time lapse full waveform inversion

Xiaohui Cai*, Kris Innanen, Qi Hu, Matt Eaid, Scott Keating, Kevin W. Hall, and Don Lawton

ABSTRACT

In order to monitor CO_2 geosequestration and CO_2 transient change. We use full waveform inversion (FWI) to quantitatively interpret the anomaly in rapid-repeat time-lapse VSP data. We present an elastic FWI workflow for indentifying and estimating time-lapse changes introduced by injection of CO_2 at a depth of 300 m, where log-derived P-wave velocity parameterization FWI, effective source estimation and time-lapse strategy are introduced. Applying the workflow to field data shows that our time-lapse inversion scheme is able to detect and quantify the time-lapse anomaly. Figure 1 show the time lapse Vp models between the monitor data and baseline data, and it indicates that the time-lapse anomaly located around 287.5 m instead of 300 m (injection location). It can be concluded that our results show that FWI of VSP data is a suitable tool for the monitoring of CO_2 transportation.

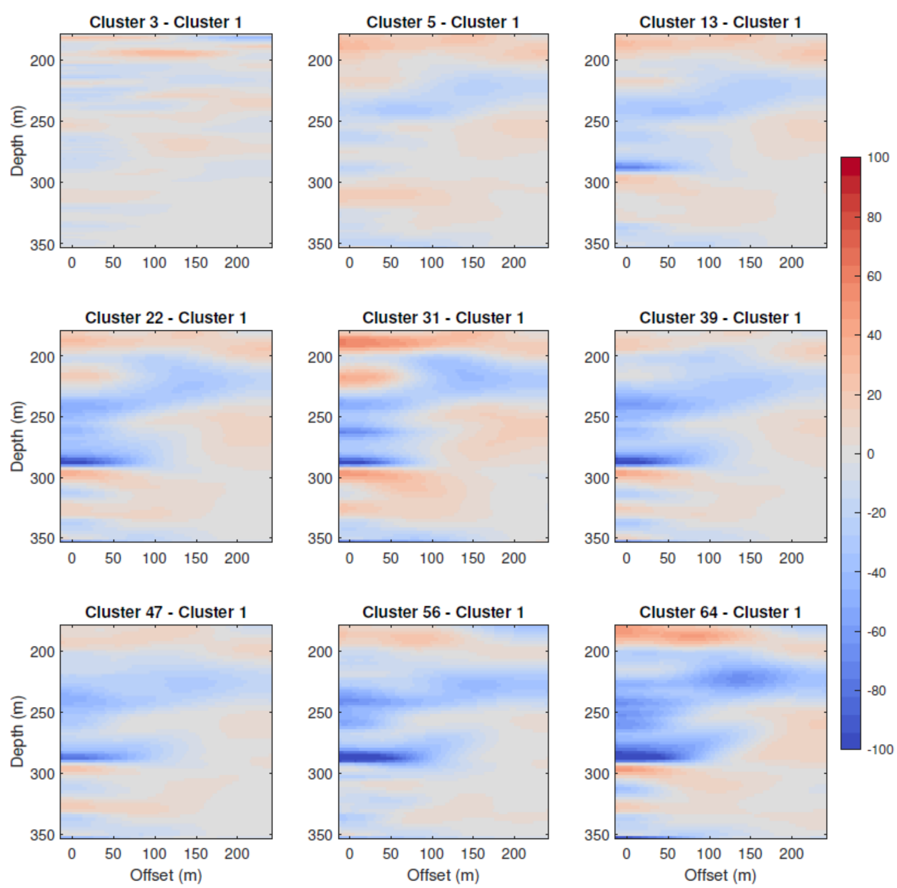

FIG. 1. The inverted V_p models difference between the 9 monitor data and baseline.

Azimuthal seismic inversion for fracture weaknesses constrained by facies

Huaizhen Chen, Jian Han, and Kris Innanen

ABSTRACT

A two-step inversion method of employing azimuthal seismic data to estimate fracture weaknesses constrained by fracture facies constraint is proposed. Firstly, based on the PP-wave reflection coefficient and azimuthal elastic impedance (EI) derived in terms of elastic properties, density and fracture weaknesses, we use a Bayesian Markov chain Monte Carlo (MCMC) algorithm to estimate EI of different incidence angles and azimuths, and predict fracture facies using the estimated EI. Secondly, we use the fracture facies to construct a more accurate initial model of unknown parameters and use the estimated EI of different incidence angles and azimuths as the input to estimate unknown parameters. Employing noisy seismic data of signal-to-noise ratios (S/N), we verify the robustness of the proposed inversion method.

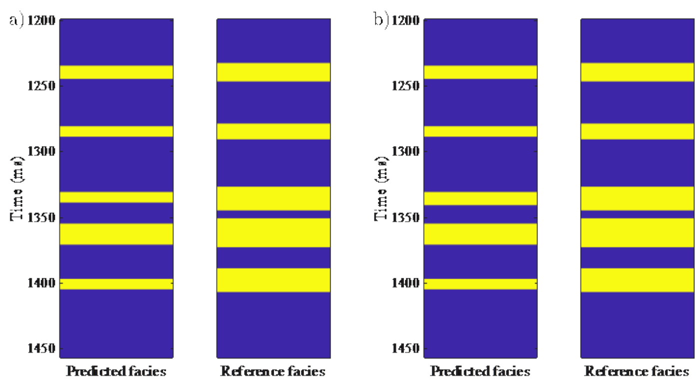

FIG. 1. a) Predicted and referenced fracture facies. a) S/N of 4; and b) S/N of 1.

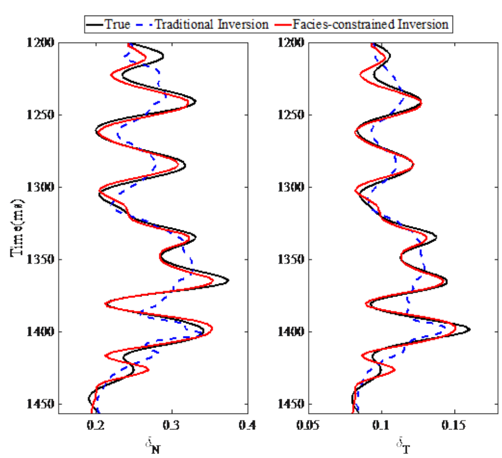

FIG. 2. a) Inversion results of fracture weakness.

Estimating reservoir parameters using first- and second-order derivatives of EI

Huaizhen Chen and Kris Innanen

ABSTRACT

Estimation of reservoir porosity, shale content and fluid type is the key and difficult problem of geophysical exploration. We relate seismic reflection coefficient and elastic impedance (EI) to reservoir porosity, shale content and fluid. Using the nonlinear reflection coefficient and EI, we present a two-step inversion method, which involves: 1) the linear inversion of partially incidence-angle-stacked data to predict EI; and 2) the nonlinear inversion of EI to estimate shale content, porosity, fluid modulus and density. We use the first- and second-order derivatives of EI with unknown parameters to improve the accuracy of the inversion for reservoir parameters. The robustness and reliability of the proposed inversion method are verified using noisy synthetic seismic data and a real data set.

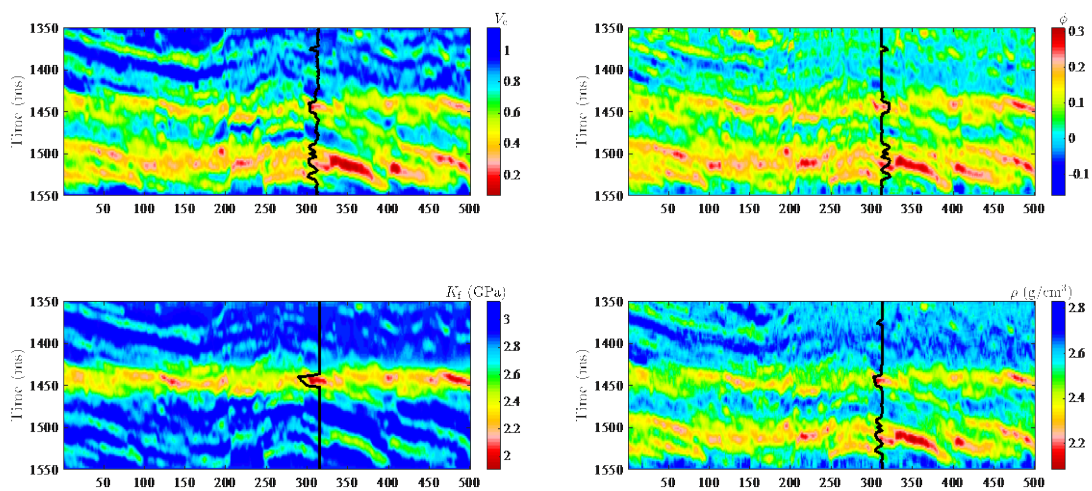

FIG. 1. Inversion results of shale content, porosity, fluid modulus and density.

Machine Learning Mineralogy Classification Comparison to Empirical Log Relationship and Implication for Physics Informed Modeling

David J. Emery*, Marcelo Guarido, and Daniel Trad

ABSTRACT

Determination of seismic lithology, porosity and pore fluid requires detailed modelling of petrophysical logs to improve the correlation with a seismic AVO response. Unfortunately, acquiring a complete set of logs for all wells in a seismic survey is unpractical, and estimating sonic, shear and density using empirical relationships is the standard approach. While these empirical relationships have worked for recon analysis, they have generally not given the details needed for accurate geophysical analysis. Machine Learning has given us a new way of investigating these relationships. By analyzing over 138 wells with DT, Vs & RHOB logs from the North Sea, Australia, and Canada, we could generate synthetic Vp, Vs, and RHOB using traditional and the XGBoost regressor, where the latter showed to work better in this data.

In the first part of this report, we intend to share our observation following log normalization & depth trend removal on DT, RHOB & DTS estimation using XGBoost (Chen & Guestrin, 2016), one of the few Machine Learning solutions that do not require completed dataset. In the second part of this report, we will look at using these empirical relationships to evaluate mineralogy. In the final part of the report, we will share some of the observations of Vp, Vs and RHOB's relationship with mineralogy.

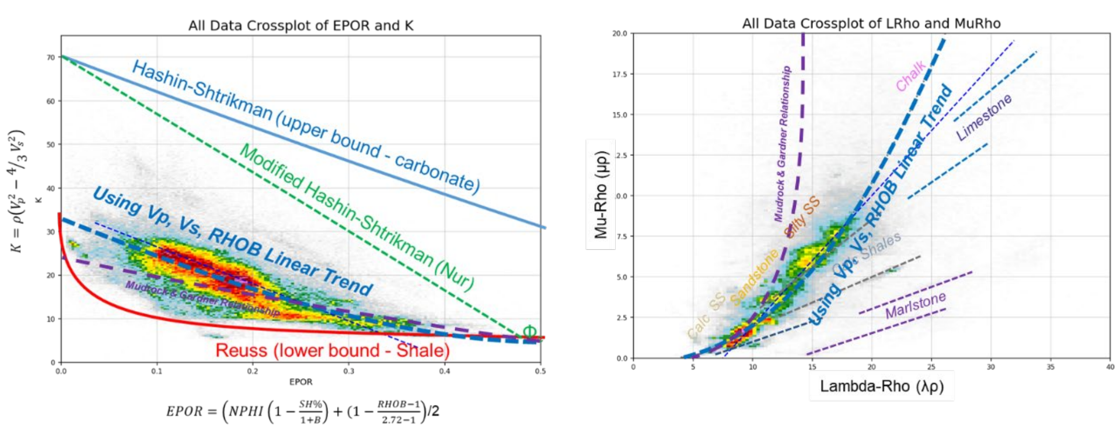

FIG. 1. Bulk Modulus (left) and Lambda-Rho/Mu-Rho (right) cross plots of input data.

The use of U-Net and Radon transforms for multiple attenuation

Paloma H. Lira Fontes*, Daniel Trad, and Ivan J. Sánchez-Galvis

ABSTRACT

Radon transform (RT) allows the mapping of multiple and primary reflection events separately in the transformed domain. Hyperbolic Radon transform (HRT) is an example of RT that maps nearly hyperbolic events in the data space to points in the HR space. A methodology of multiple prediction is proposed based on U-Net, a convolutional neural network (CNN) architecture. This network is often applied to image segmentation for classification problems, but the proposed workflow uses the U-Net to predict multiples using HR panels. In this report, we performed predictions using one or two input channels, sparse and nonsparse HR panels, with nonsparse HR panels of multiples as the label. These numerical experiments show that a U-Net can be used to separate the primaries and multiples in the Radon space and therefore predict multiples. This result was achieved using simple geologic models, but further work is required with more complex geologic models. A challenging aspect of this problem is that the transform generates artifacts that are very dependent on the geometry of the input (truncation and sampling artifacts). Because these are very difficult to predict at inference time, they cause a decrease in generalization power.

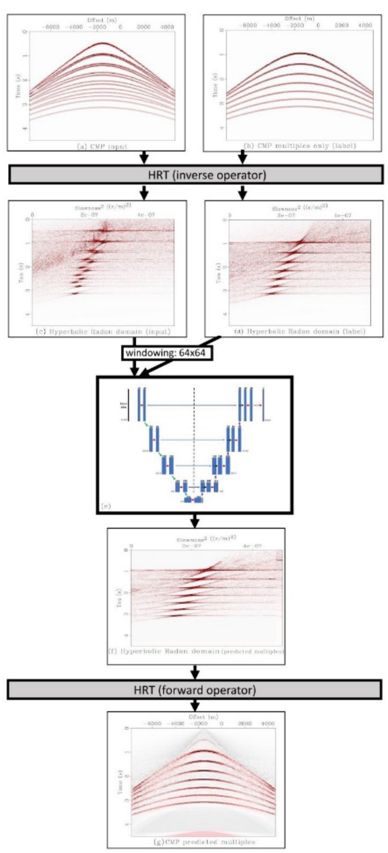

FIG. 1. One channel workflow to predict multiples using HRT.

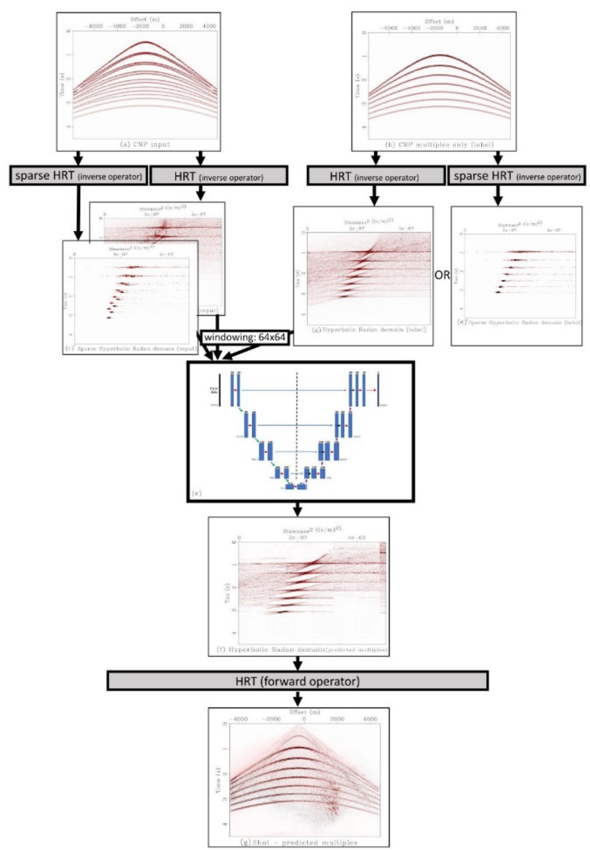

FIG. 2. Two channels workflow to predict multiples using sparse and nonsparse HRT.

Non-repeatability effects on time-lapse elastic full-waveform inversion for VSP seismic data

Xin Fu*, Kris Innanen, Scott Keating, and Qi Hu

ABSTRACT

In this study, we investigate non-repeatability effects on time-lapse elastic full-waveform inversion for VSP (vertical seismic profile) seismic data. The non-repeatabilities tested are the non-repeatability on source locations, the non-repeatability on random noises, and the non-repeatability on the near-surface properties. Four time-lapse inversion strategies, including the parallel strategy (PRS), the sequential strategy (SQS), the double-difference strategy (DDS), and the common-model strategy (CMS, are applied in each type of non-repeatability. From the investigation, we can conclude: P-wave velocity changes can be better recovered than S-wave velocity changes; except for the DDS, the other three strategies have similar performance; the DDS also has similar performance to the others when acquisition geometries for baseline and monitor surveys are identical, but it is sensitive to the non-repeatability on source locations between twice surveys; no strategies can effectively handle the case of random noise; near-surface property changes have limit impact on the recovery of time-lapse changes for VSP data.

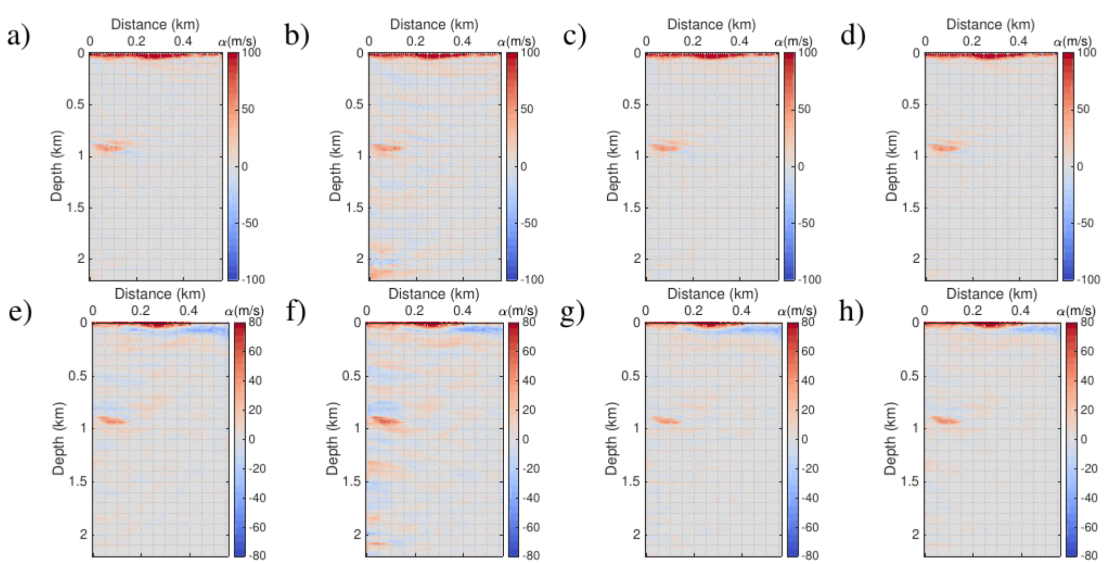

FIG. 1. Inverted results of the time-lapse changes with near-surface property changes in the case that baseline and monitor surveys are perfectly repeated. The first row is the inverted P-wave velocity changes of the PRS (a), the SQS (b), the DDS (c), and the CMS (d). The second row is the inverted S-wave velocity changes of the PRS (e), the SQS (f), the DDS (g), and the CMS (h).

A robust source-independent full-waveform inversion

Xin Fu and Kris Innanen

ABSTRACT

Full-waveform inversion (FWI) can reconstruct high-resolution underground velocity and lithology structures even under complex geological backgrounds, and has been widely developed. But a reliable real-data inversion generally needs accurate source wavelet information, which is still one of the major challenges in FWI. In this paper, a robust source-independent FWI method is developed, which is demonstrated via synthetic tests of different starting models, different true models, different levels of random noises, and different types of source wavelets. It does not require any prior source wavelet information. It does not require an accurate starting model, even a 1D starting model is feasible to output an accurate wavelet estimate. It is stable for random noises. A good estimate of the source wavelet can be obtained from a poorly converged model based on the new proposed wavelet estimation equation. All in all, the performance of the new source-independent FWI in the synthetic data tests is close to that of the known-source-wavelet FWI.

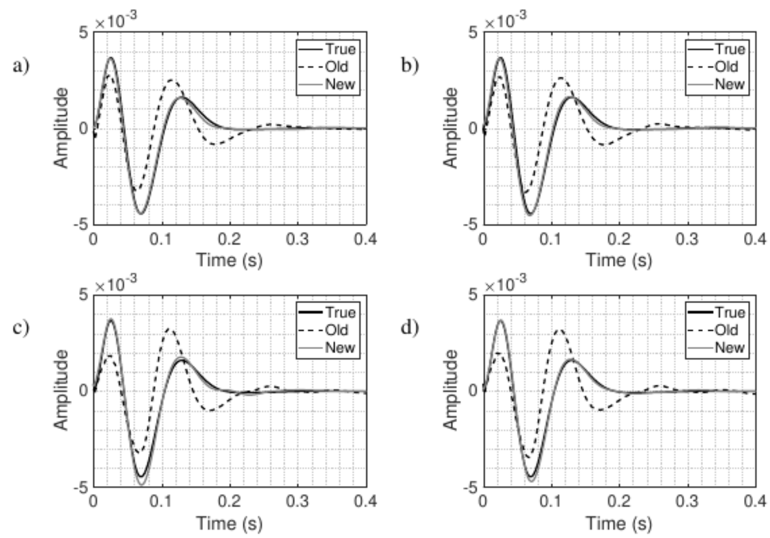

FIG.1. The final estimated source wavelets of the old method and the new method using starting models 1 (a), 2 (b), 3 (c), and 4 (d), respectively. In each panel, the black line is the true source wavelet, the dashed line is estimated from the old method, and the gray line is estimated from the new method.

Time-lapse full-waveform inversion for cases with seawater or near-surface velocity changes

Xin Fu and Kris Innanen

ABSTRACT

Time-lapse (4D) seismic full-waveform inversion (FWI) can provide high-resolution imaging of reservoir changes caused by the production of hydrocarbon (e.g., enhanced oil recovery) and the unground storage of CO_2. However, successful seismic monitoring depends on good repeatability between baseline and monitor surveys. However, the capacity of time-lapse FWI technology on solving the non-repeatability issue of seawater or near-surface velocity changes during baseline and monitor seismic surveys has not been demonstrated. In this paper, we investigate the capability of the parallel strategy, the double-difference strategy, the sequential strategy, and the common-model strategy in the non-repeatability issue of seawater or near-surface velocity changes using synthetic time-lapse marine streamer data, time-lapse OBN (ocean-bottom node) data, and time-lapse surface land data. The investigation shows that when using marine streamer data, both the double-difference strategy and the common-model strategy can adapt to relatively small seawater changes, and only the common-model strategy can adapt to relatively big seawater changes; when using OBN data, the parallel strategy, the double-difference strategy, and the common-model strategy all can adapt to relatively small seawater changes, and the best result is given by the double-difference strategy, but none of them can adapt to relatively big seawater changes; when using surface land data, the common-model strategy can adapt to the random near-surface changes best.

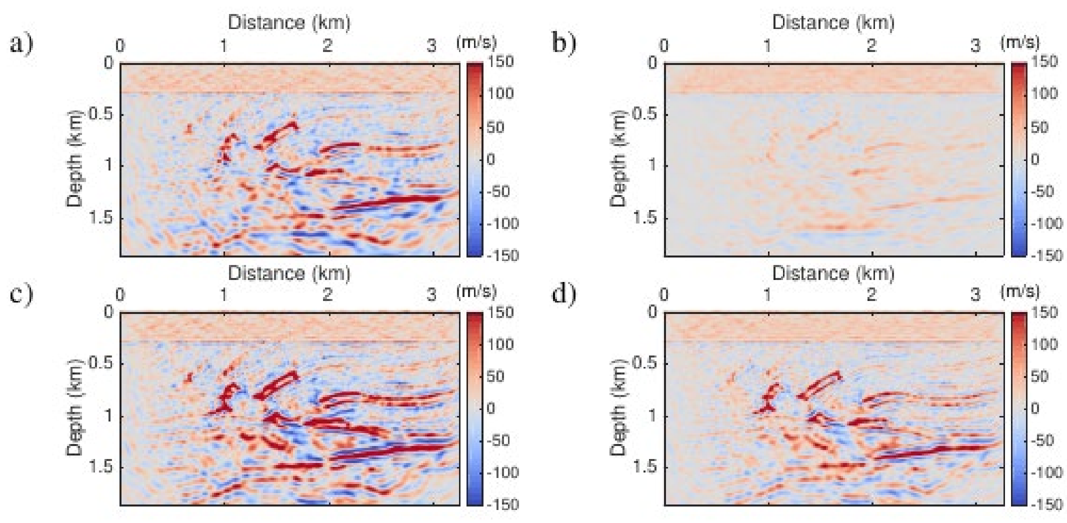

FIG.1. The inverted time-lapse changes of various strategies from OBN seismic data for the marine time-lapse model with a 50m/s seawater velocity change. (a) the parallel strategy, (b) the double-difference strategy, (c) the sequential strategy, and (d) the common-model strategy.

Time-lapse full-waveform inversion for ocean-bottom node seismic data with seawater velocity changes

Xin Fu and Kris Innanen

ABSTRACT

As a powerful tool for 4D seismic data inversion to monitor subsurface reservoir changes and/or CO_2 storages, full waveform inversion (FWI) has the ability of high-resolution imaging of physical properties for subsurface media, and it can solve the problem of non-repeatable receiver/source positions in time-lapse seismic surveys. In this report, we develop a three-stage time-lapse (TTS) FWI strategy for ocean-bottom node seismic data, in which the first stage is to use FWI to estimate the seawater velocities in the baseline model and the monitor model, respectively; the second stage is to obtain a relatively good common starting model that is close to the final inversion result, to guide the next baseline FWI and monitor FWI to converge to local minima that are closing to each other; the third stage is to employ the better starting models acquired in the second stage to carry out the final convergence and reflect the time-lapse differences. The tests using synthetic data obtained from acoustic models with different levels of seawater velocity changes have demonstrated the feasibility and stability of our new method.

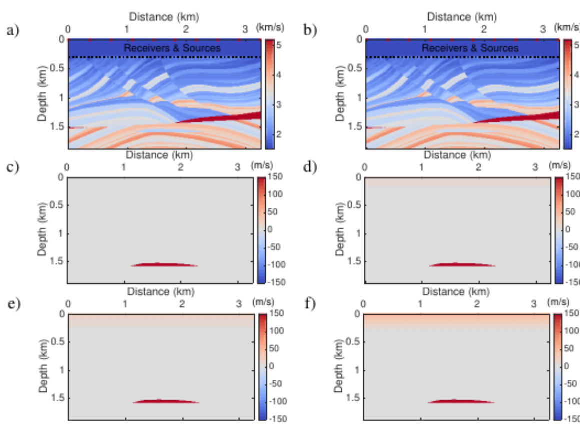

FIG. 1. ((a) Baseline model. (b) Monitor model. (c) Time-lapse change 1 without seawater velocity change. (d) Time-lapse change 2, the maximum seawater velocity change is 10m/s. (e) Time-lapse change 3, the maximum seawater velocity change is 20m/s. (f) Time-lapse change 4, the maximum seawater velocity change is 50m/s. The seawater velocity change is decreasing with depth.

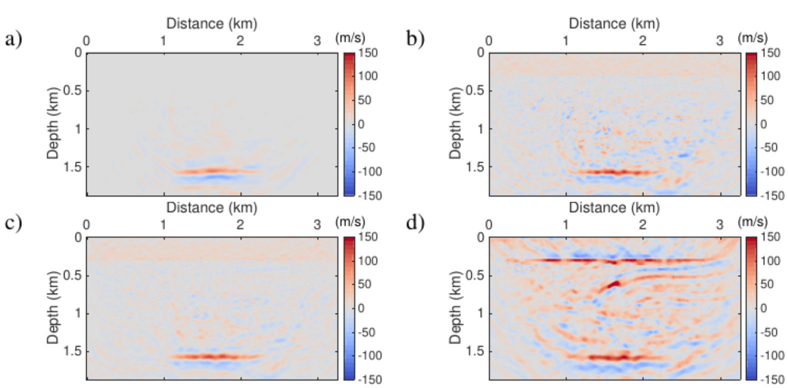

FIG. 2. Inverted time-lapse changes of the TTS of true time-lapse changes (a), (b), (c), and (d) are, respectively, time-lapse changes

Oil Spills Identification on Satellite Radar Data with Deep Learning

Marcelo Guarido, David J. Emery, Daniel Trad, and Kris Innanen

ABSTRACT

Oil spills in oceans are a major pollutant endangering oceanic and coastal marine life, and their detection is of high environmental importance. Manually detection presents a challenging and lengthy task. We presented a deep learning model based on the U-Net structure to identify oil bodies in satellite radar images with promising results. Our model successfully classified larger oil bodies with moderate success on smaller ones. Image feature engineering, such as a four-directional cumulative, brought important information to the model and performed more accurate predictions. Limited by computer resources, our model was relatively simple. We used pre-trained weights from the MobileNetV2 model. Although initial results are unsatisfactory, we will continue to explore the transfer learning methodology to generate more accurate oil detection algorithms.

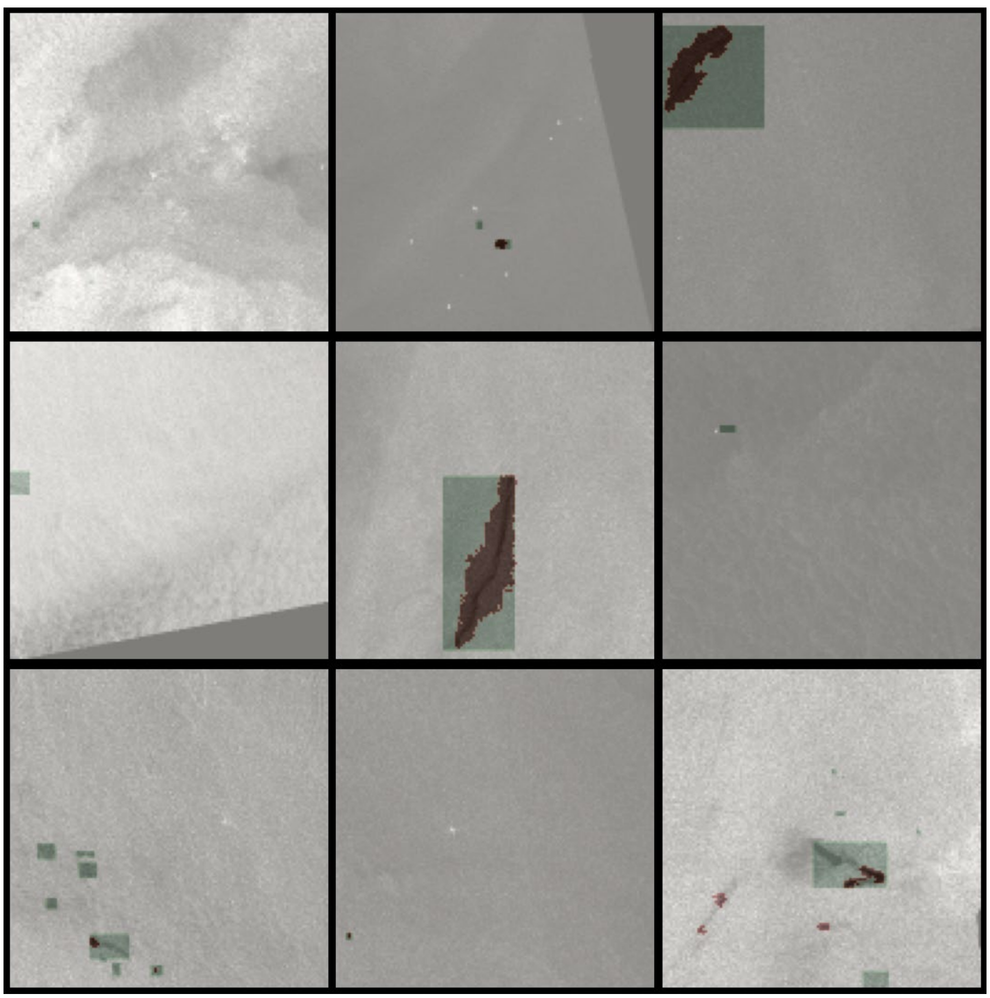

FIG. 2. True mask in green and predictions in red. The model seems to work better on significant events.

Using Natural Language Processing to Convert Mud-Log Chip Descriptions to Useful Data Tables

Marcelo Guarido*, David J. Emery, and Kris Innanen

ABSTRACT

We successfully created a natural language processing pipeline to extract mud-logging cutting descriptions from PDF files. We converted them to usable structured numerical tables that can be used to match with wireline logs or seismic sessions. The nature of the original tables required extensive preprocessing of the extracted object, including data manipulation, pattern recognition, missing values treatment, and resample. The extract and processed table were merged with well logs and used to predict DTC and provided important improvement of the predictions compared to the baseline model using wireline logs only, where the R2 improved from 0.73 to o.82 using a linear regression model. Feature selection with the stepwise regression generated an optimized model that kept the quality of the predictions and used logs and cutting descriptions with equal importance. Lately, an XGBoost regressor created a non-linear model to improve the predictions with an R2 of 0.88, relying more on the wireline logs. New tests were done on a train-validation split of 5% and 95% to avoid biased predictions. Both the stepwise and XGBoost regression predictions were less precise but still close to the actual values, showing the robustness of the methodology.

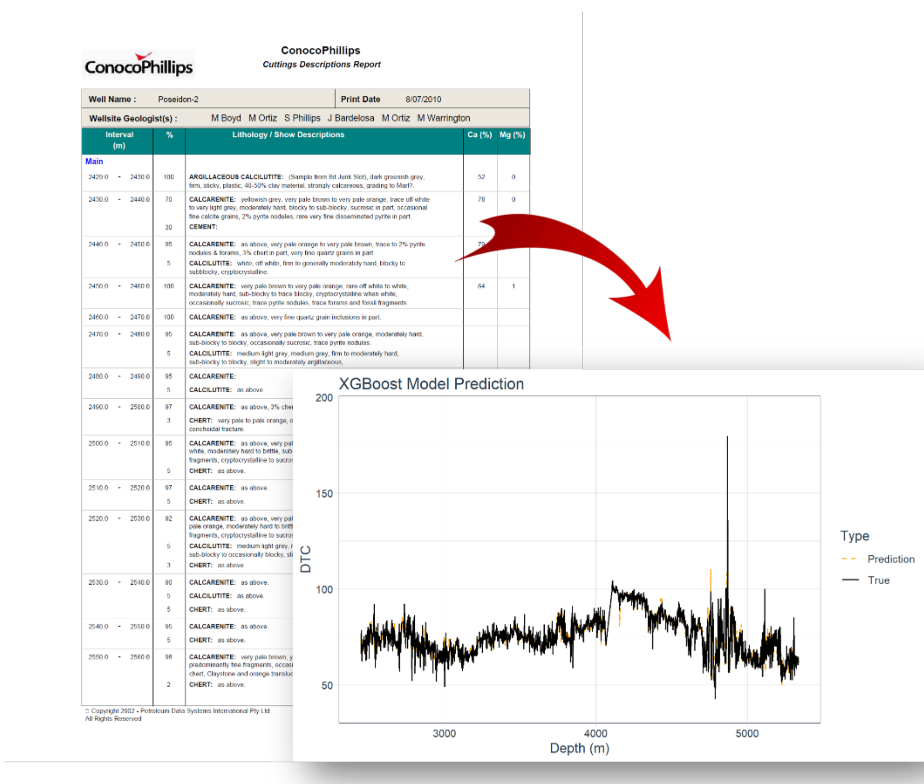

FIG. 3. PDF table to DTC prediction.

The croissant: a smaller, fluffier, flakier pretzel

Kevin W. Hall*, Kris Innanen, and Don Lawton

ABSTRACT

While we have a working experimental directional DAS sensor (DDS) at Carbon Management Canada's Newell County Facility, it is quite large (10x10m), and being horizontal and flat, has no way to record vertical component data (Hall et al., This volume). Logistically, we need a smaller sensor that can record vertical motion and is easier to bury for permanence and coupling. Testing (Figure 1) has shown that we can record reasonably consistent data on a sensor where the one-meter-long sides of the sensor are smaller than the default seven-meter gauge length used in our DAS interrogator (Figure 2). In future, after further testing, we plan to install a receiver line containing more than one directional DAS sensor at the Facility.

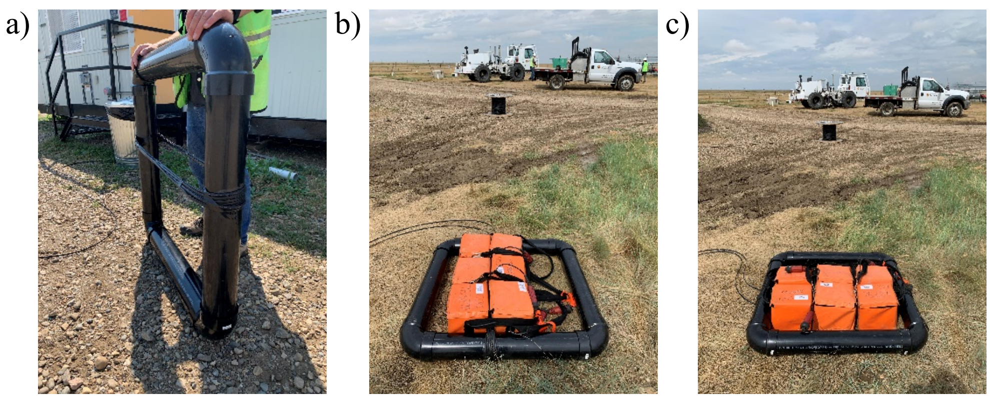

FIG. 1. Test 2: A 1x1 m frame was wrapped with 14 m of fiber cable (a) and placed flat on the ground with the fiber oriented in-line (b) and cross-line (c) 22.6 m from the Vibe. Coupling was provided by stacking batteries on top of the fiber. The remainder of the fiber was left on the spool, which was placed 15.6 m from the VP with the axis of the spool oriented vertically.

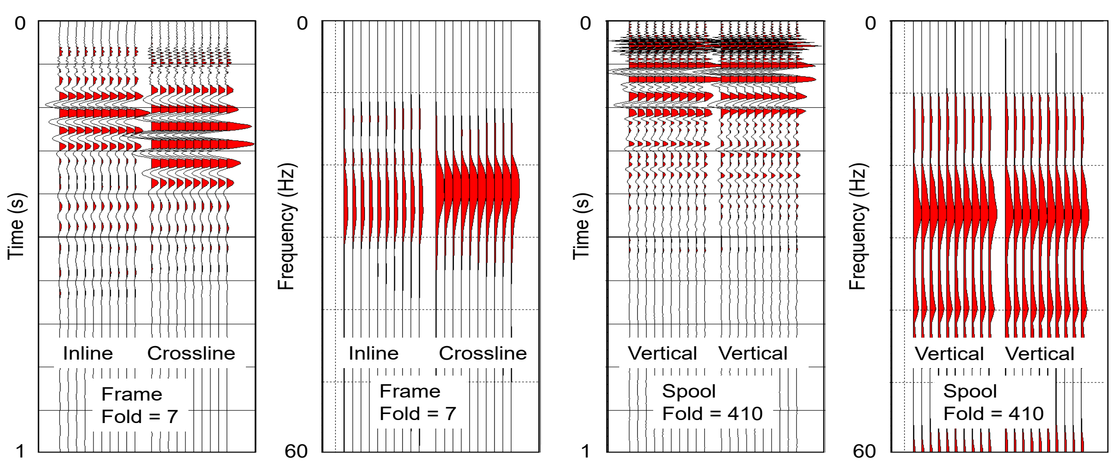

FIG. 2. Stacked and correlated data recorded for Test2 sweeps with fiber on the frame oriented in-line (a), and cross-line (b) relative to the Vibe location (cf. Figure 5). Figure 7c shows stacked traces and amplitude spectra from the frame and spool repeated 10 times for visibility.

Cvictus VSP

Kevin W. Hall and Kris Innanen

ABSTRACT

CREWES participated in the acquisition of walk-away baseline and monitor crosswell and vertical seismic profile (VSP) surveys at a Cvictus combined hydrogen production and carbon dioxide sequestration site in central Alberta in early 2022. Fifteen hundred tons of CO_2 were injected between the baseline and monitor surveys. Distributed acoustic sensing (DAS) data were acquired for downhole sparker data over a 150 m depth interval for the cross-well baseline survey and a 38 m interval for the cross-well monitor survey with a nominal twelve shots per depth level. Vibe points (VP) on four different azimuths centered on the observation well were acquired with eight sweeps per VP for the baseline VSP and sixteen sweeps per VP for the monitor survey. Initial time-lapse zero-offset VSP processing of a single VP shows no obvious post-injection amplitude or time-delay anomaly at reservoir depth. More work, including modelling and full processing of the walkaway VSP's is in progress.

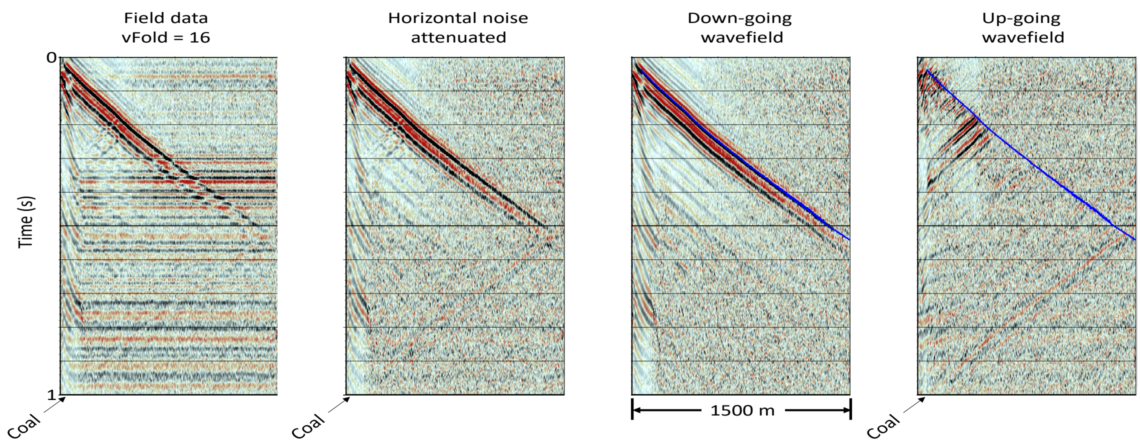

FIG. 1. Monitor survey VP 2010 wavefield separation using a *f-k* pie-filter with 8 km/s cut-offs.

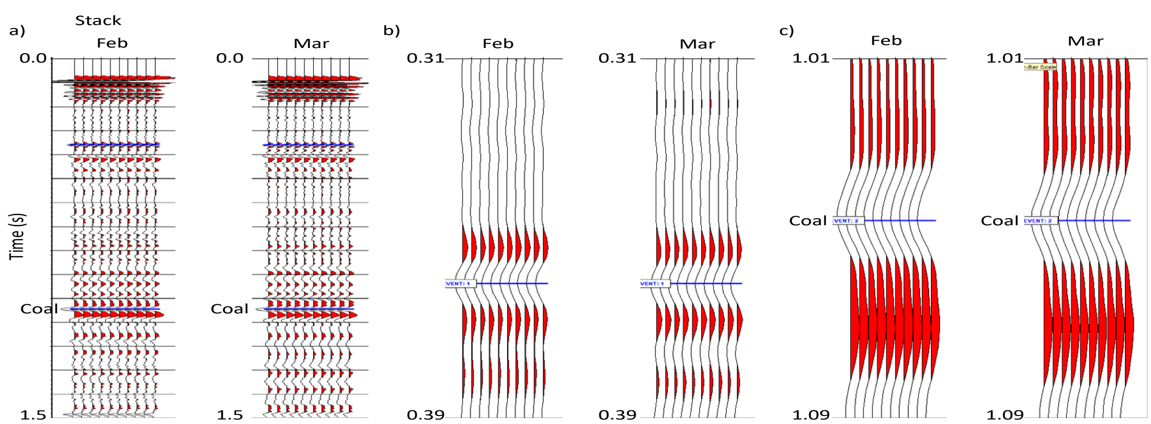

FIG. 2. Comparison on monitor and baseline VP2010 stacks after flattening on first-break picks and applying a top mute: (a) 0-1.5 s, (b) 0.31-0.39 s, and (c) 1.01-1.09 s.

Multi-azimuth and offset directional strain tensor results recorded on an experimental directional DAS sensor

Kevin W. Hall, Kris Innanen, and Don Lawton

ABSTRACT

An experimental 10x10 m Directional DAS Sensor (DDS, also known as the Pretzel) was buried at a depth of 2 m at Carbon Management Canada's Newell County Facility (formerly known as the Containment and Monitoring Institute's Field Research Station, or CaMI.FRS), near Brooks Alberta in 2018, and 4 VP were recorded for testing. We recorded 549 VP on the sensor as part of the Snowflake2 survey that was acquired in 2022. The data were processed to extract traces from the center of each side of each square in the sensor to form eight component source gathers, followed by estimation of NN, EN and EE directional strain tensor traces. We plot time slices of the results as colour-coded quiver plots in map form where the base of the quivers are located at VP-DDS mid-point locations, and have observed circular wavefronts propagating with an apparent direction from the DDS towards far offsets (Figure 1). The results presented in this report constitute a better, and certainly more complete, proof of concept demonstration of the DDS than was previously possible.

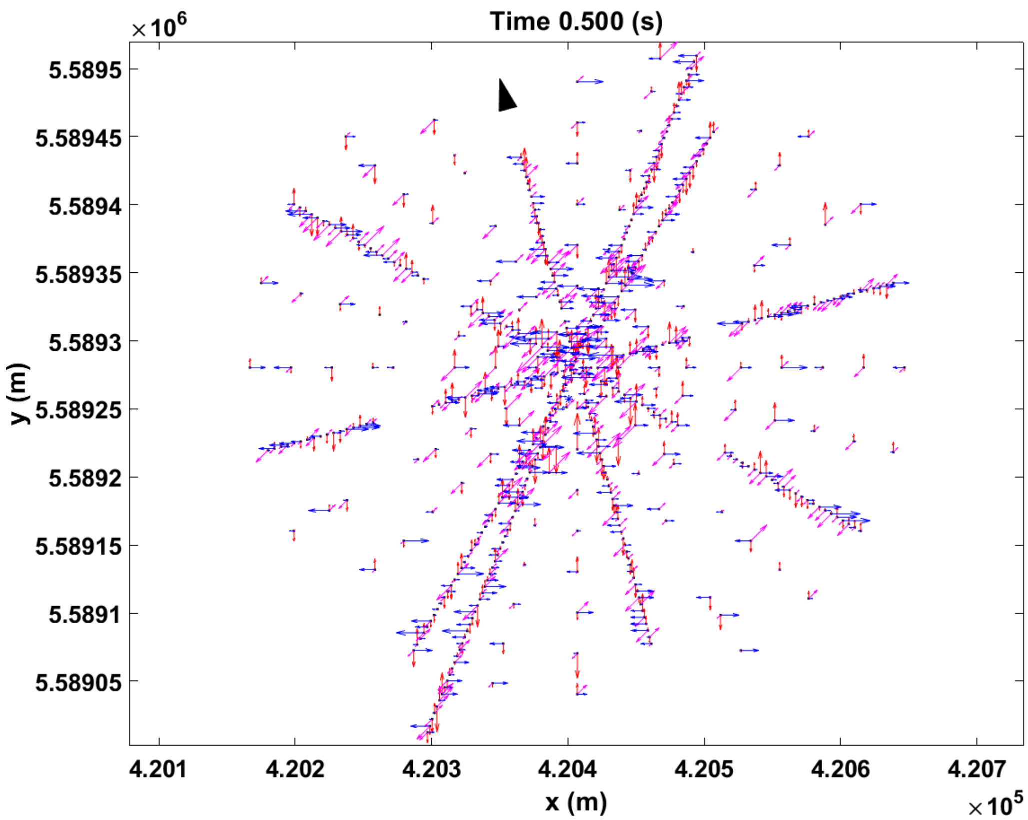

FIG. 1. Matlab quiver plot for a time-slices at 0.5 s of three component directional strain traces. The base of the quivers are located at midpoint locations between each VP and the DDS. Map co-ordinates have been rotated 15 degrees counterclockwise around the DDS location for display.

Shadow imaging: attenuation projection of acoustic waves from a circular array without arrival picking

David C. Henley

ABSTRACT

Seismic physical modeling systems can be used to record acoustic and elastic wavefields for a wide variety of situations of interest not only to seismologists, but to other professionals, as well. We demonstrate here a novel processing scheme for the transmitted acoustic amplitudes measured by coincident circular arrays of ultrasonic receivers and sources, immersed in the tank of the CREWES physical modeling system.

Most processing techniques for transmitted acoustic waves rely on a 'picked' acoustic 'arrival' to yield the transit time for a pulse traveling along each assumed raypath. A family of techniques, usually called 'tomography', can be applied to provide a low-resolution image of object(s) immersed within the circular acquisition aperture. Tomographic methods which use arrival times provide a 'delay time' or velocity image of the aperture and included object(s). The images are very sensitive to errors in the time picks.

We demonstrate, instead, a form of tomographic imaging which does not rely on explicit time picks of acoustic wave arrivals, but instead on much less sensitive acoustic magnitudes, or envelope amplitudes, selected at consistent points on each acoustic record. The smoothed envelope amplitude, or magnitude, is inversely proportional to the attenuation along each transmission path. We term our technique 'shadow imaging', since it orients the 'attenuation shadow' observed from each source around the array, and stacks the oriented shadows to form an attenuation image (a form of projection tomography).

Figure 1 shows the trial attenuation shadow image for the 35 source positions in our experiment, stacked over common image aperture coordinates.

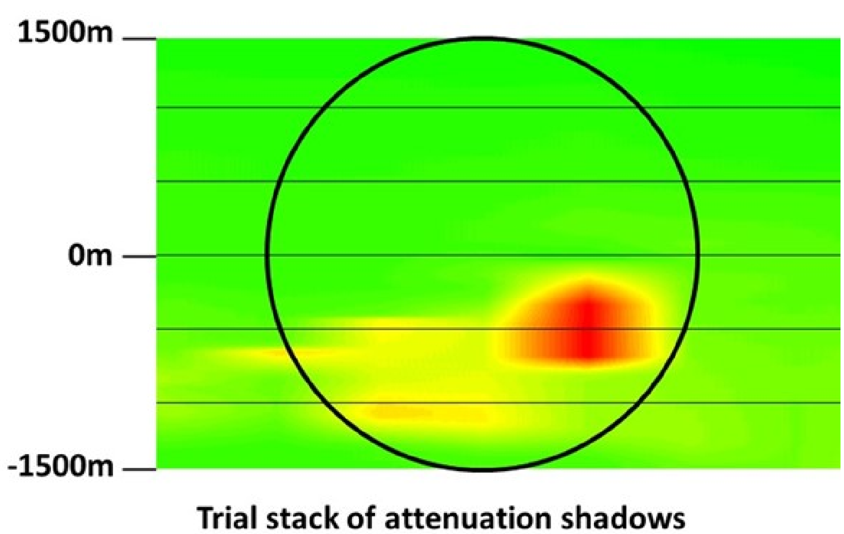

FIG. 1. Source attenuation shadows stacked over image coordinates.

A Novel Data Science Approach to Borehole Dysfunction Analysis

Scott Hess*, Roman Shor, Kris Innanen, and Alex Vetsak

ABSTRACT

During drilling activities, monitoring the quality of the borehole is an essential task. Borehole dysfunctions such as constrictions, ledges, and differential sticking can cause significant amounts of non-productive time that decreases overall operational performance. The dysfunctions are most troublesome during tripping operations when the drill string is moved in and out of the borehole. Identification of dysfunctions before significant operational issues occur, such as stuck pipe, can allow proactive mitigating actions to reduce the impact on the tripping operation. Modelling methods for expected sliding friction for good borehole conditions provide a baseline for hook load operating parameters during tripping out of the borehole. Assuming the baseline hook load estimation is somewhat accurate, the anomalous high hook loads above baseline, referred to as overpull, provide measurements that should capture the resistance in the borehole due to dysfunctions. The focus of this study is to utilize overpull signatures and the drill string configuration to produce a resistance depth profile that can provide better depth resolution to place dysfunctions along the wellbore and also characterize the dysfunction mechanism. This paper represents the initial steps of developing a forward modelling strategy using a source signal (i.e. the drill string) convolved with a resistance signal (i.e. the dysfunctions) to produce overpull signals. Initial tests show promising similarities compared to overpull real data.

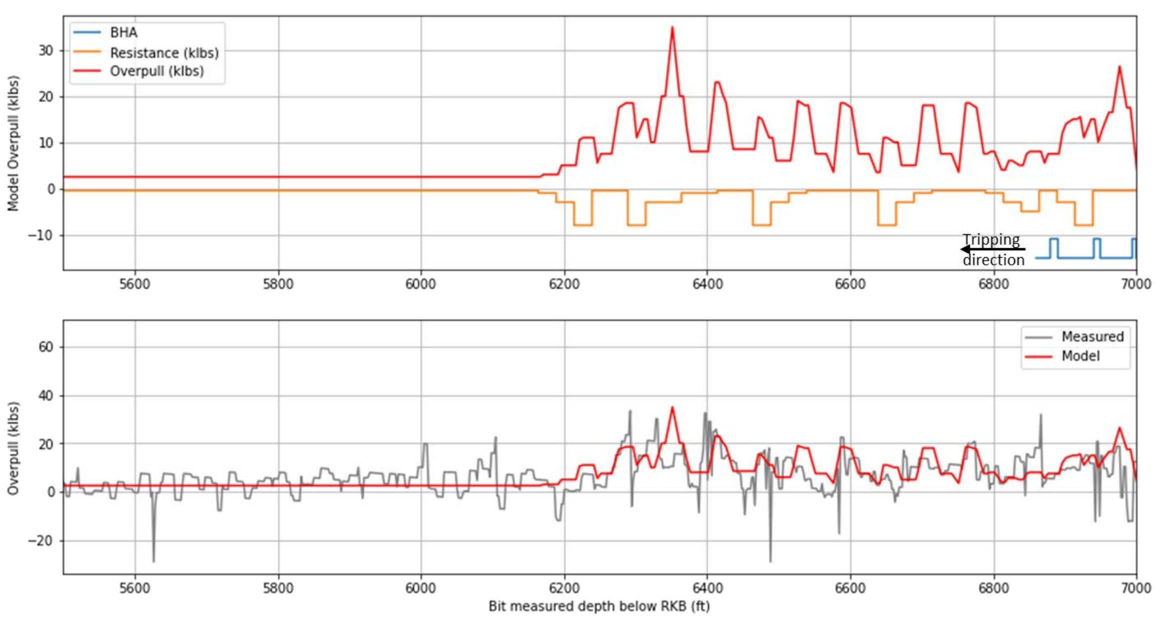

FIG. 1. The model overpull (green) is calculated by convolving the BHA source signal (blue) with the resistance signal (orange) starting from the maximum depth of the borehole. Similar overpull signatures can be observed in the model and a real dataset (red), specifically the overpull between approximately 6300ft and 7150ft.

Bayesian approaches to estimating rock physics properties from seismic attributes

Qi Hu and Kris Innanen

ABSTRACT

Bayesian rock physics inversion refers to a set of probabilistic methods for the prediction of reservoir properties from elastic attributes, based on different statistical assumptions for the distribution of the model variables and different linear or nonlinear rock physics models. We have examined three Bayesian approaches using the well-log data at the Carbon Management Canada Newell County Facility, assuming Gaussian, Gaussian mixture, and non-parametric distributions of the rock physics variables. The solution is represented by the posterior distribution of the porosity and lithology parameters conditioned on the elastic data. In this application, because the nonlinearity of the rock physics model is not strong and the data are approximately Gaussian distributed, the three results are similar, all capturing the trend of the actual logs. However, the Gaussian mixture model might be a more appropriate solution, owing to its efficiency and its ability to recognize the multimodality of the data. The proposed methods can be combined with elastic inversion to implement a two-step workflow of seismic reservoir characterization at the field if we assume that the rock physics model calibrated at the well location is also valid far away from the well.

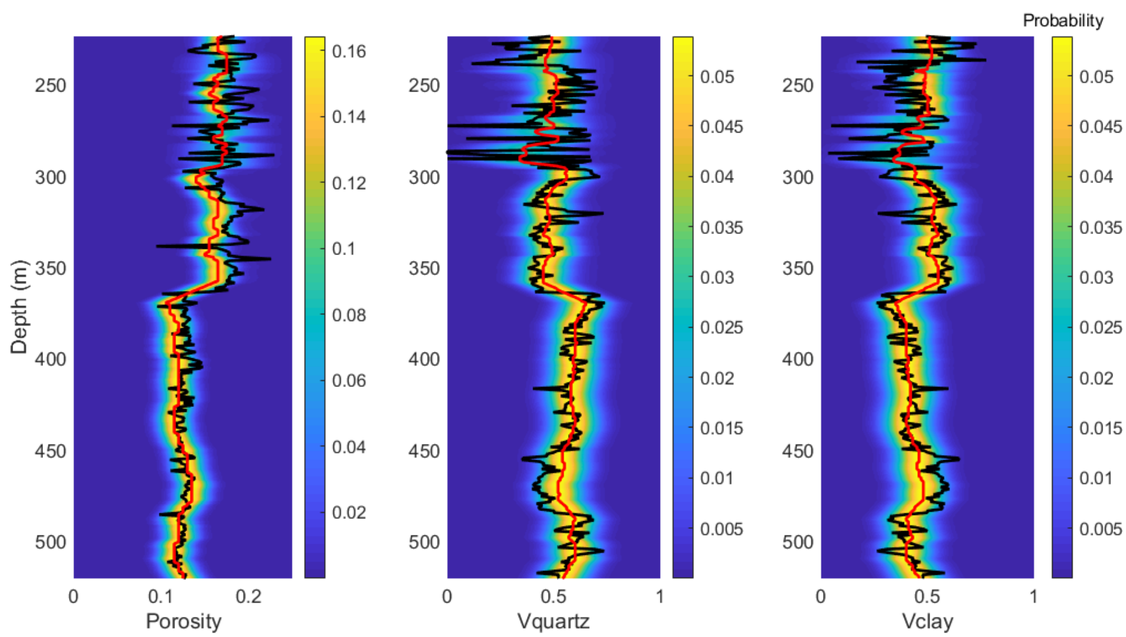

FIG. 1. Results of the Bayesian Gaussian mixture rock physics inversion. The background color represents the posterior distribution and the solid red curves represent the maximum a posteriori predictions. The solid black curves represent the actual well logs.

Quantitative FWI characterization and monitoring of reservoir properties at the CMC Newell County Facility

Qi Hu*, Matt Eaid, Scott Keating, and Kris Innanen

ABSTRACT

The spatial distribution of CO2 saturation and the plume location can be monitored using time-lapse seismic data. Due to the limited knowledge of rock and fluid properties before injection, model predictions are often uncertain and must be updated when new measurements are available. The 2018 CMC VSP survey provided a dataset suitable for creating a baseline subsurface model for later monitoring studies. In this report, we apply full waveform inversion to the measured data, to reconstruct the subsurface model of elastic and rock physics properties. The key strategies used in our FWI framework are the effective source method for coping with near surface complexity, the inclusion of DAS data in FWI for leveraging the complementary aspects of accelerometer and DAS data, and the rock physics parameterized FWI that allows for jointly updating the elastic and rock physics variables. The result is high-resolution, plausible, and has good agreement with the well-log data.

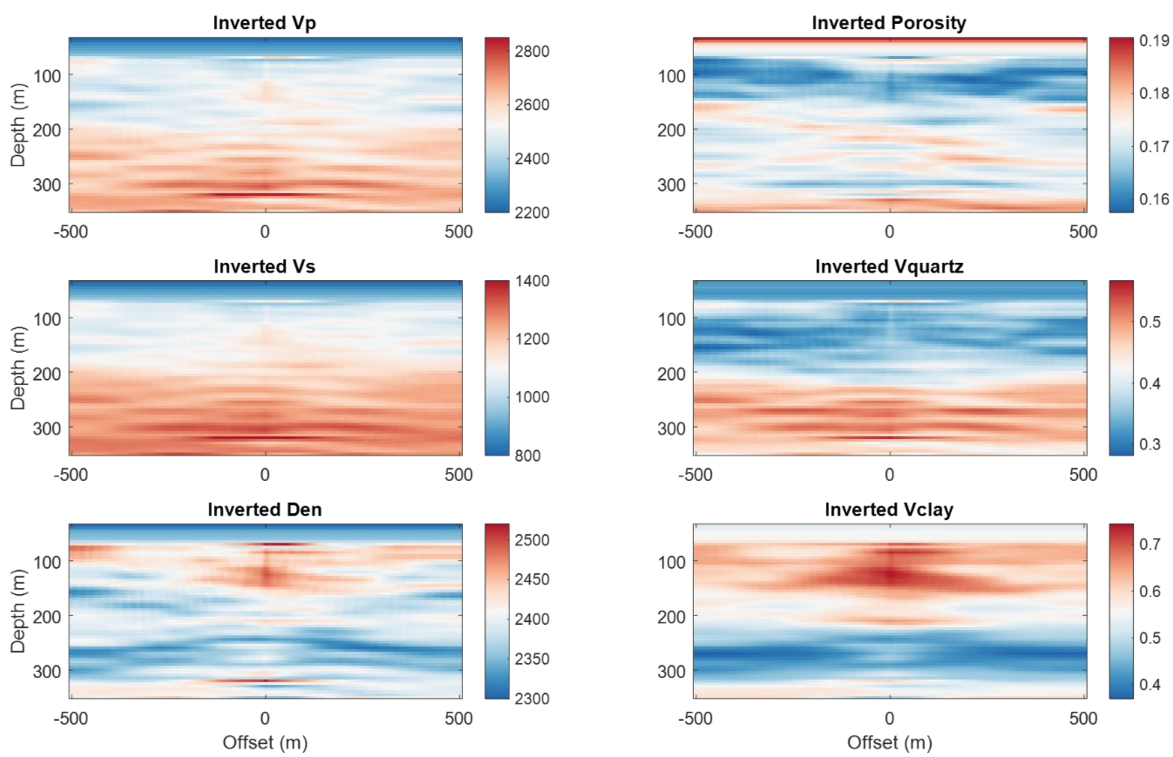

FIG. 1. Recovered elastic and rock property models with direct rock physics FWI.

Time-lapse FWI prediction of CO_2 saturation and pore pressure

Qi Hu* and Kris Innanen

ABSTRACT

The estimation of CO_2 saturation and pore pressure from time-lapse seismic data requires a physical model relating the variations in reservoir properties to the changes in seismic attributes. We propose a complete rock physics workflow combing Macbeth's model and Gassmann's equations to predict elastic properties as a function of porosity, mineralogy, saturation, and pressure. We validate this workflow using a published dataset. In particular, we demonstrate the advantages of Macbeth's model in predicting the effect of pressure changes. Furthermore, we propose a full waveform inversion (FWI) algorithm incorporating the proposed model for the prediction of the time-evolution of CO_2 saturation and pore pressure. This approach allows for direct updating of reservoir properties from seismic data. We derive static rock properties, such as porosity and clay content, from baseline data and use them as input to predict dynamic reservoir properties (saturation and pressure) from monitor data. We illustrate the potential of the approach using a synthetic time-lapse dataset.

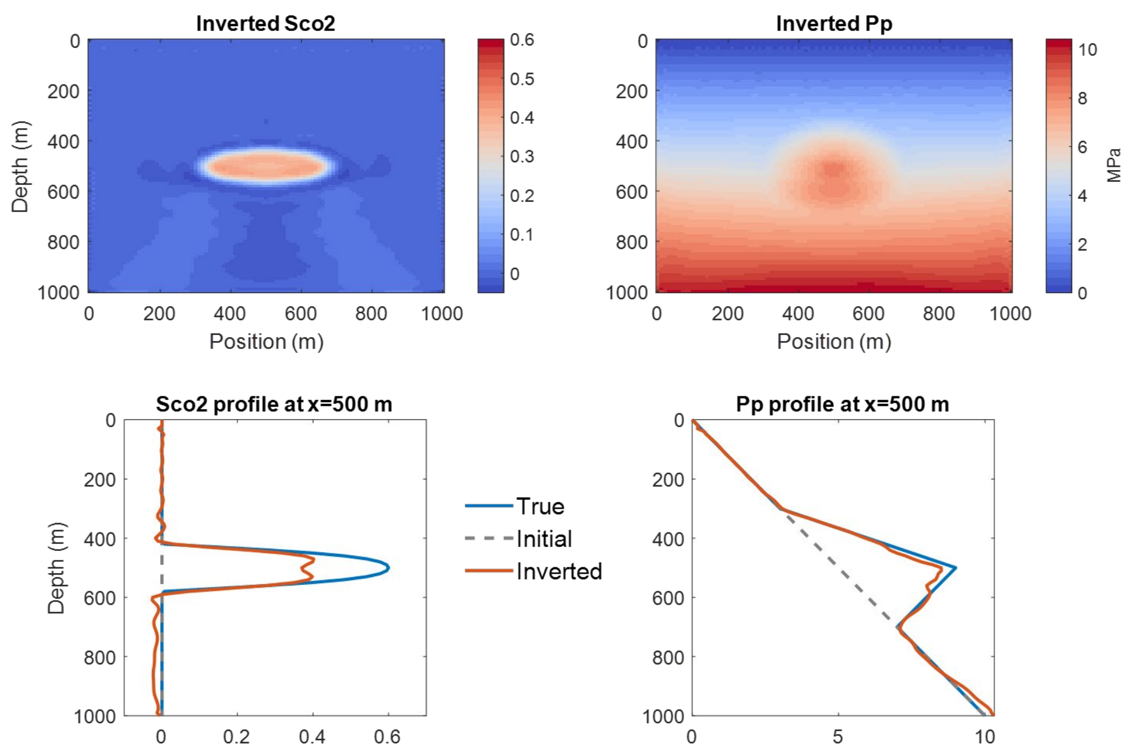

FIG. 1. Recovered monitor model of CO2 saturation and pore pressure.

Discrete wavelet transform application in a CNN-based reverse time migration with multiple energy

Shang Huang and Daniel Trad

ABSTRACT

In seismic imaging, image resolution and accuracy are affected by migration approaches. Deep learning has recently been considered an alternative and efficient way to improve image quality. In this project, discrete wavelet transform (DWT) is applied with U-Net on migration data containing multiple energy. The neural network approximates the inverse of the Hessian to obtain high-quality reflectivity prediction. Results show that the DWT subband helps the model learn smooth input, extract critical features from data, and enhance image resolution. Multiple energy provides valuable information for subsurface structure expanding prediction illumination.

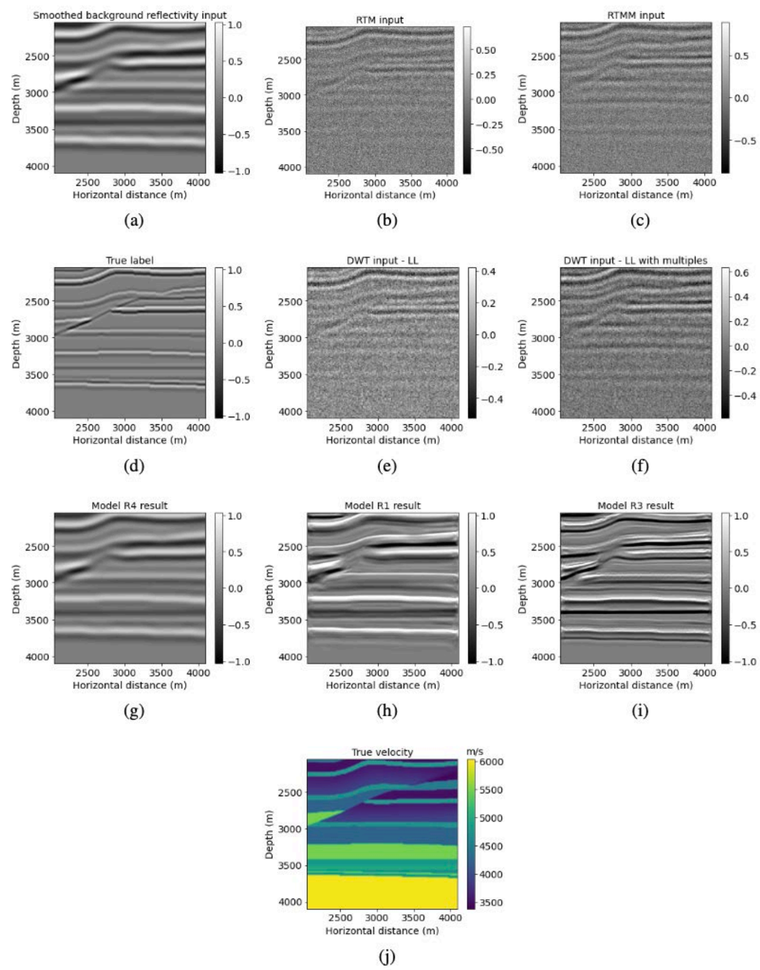

FIG. 1. Overthrust example 2 results after adding noise. (a) Reflectivity from the background velocity, (b) true windowed band-limited reflectivity, (c) RTM image without multiple energy, (d) true label, (e) DWT subband LL without multiple energy, (f) DWT subband LL with multiple energy, (g) model R4 result based on workflow 4, (h) model R1 result based on workflow 1, (i) model R3 result based on workflow 3, and (j) true windowed velocity.

Time-lapse monitoring using neural networks

Shang Huang* and Daniel Trad

ABSTRACT

Time-lapse seismic monitoring quality is affected by near-surface noise, weak reservoir changes amplitude and poor subsurface illumination. Except for some geophysical approaches, deep learning can solve the challenges above with high efficiency and accuracy. This project uses a stacked bidirectional long short-term memory neural network (SD-Bi-LSTM) to predict near-surface noise from baseline seismic data. A U-Net is then followed to work on image residuals to suppress noise on a large scale. Furthermore, the surface multiple is added in forward modeling to generate baseline and monitor data with expanded subsurface illumination. Results show that SD-Bi-LSTM can predict and mitigate noise in monitor data. The final difference between baseline and monitor models has suppressed significant noise after combining SD-Bi-LSTM, U-Net and surface multiples. Images have improved accuracy and high quality.

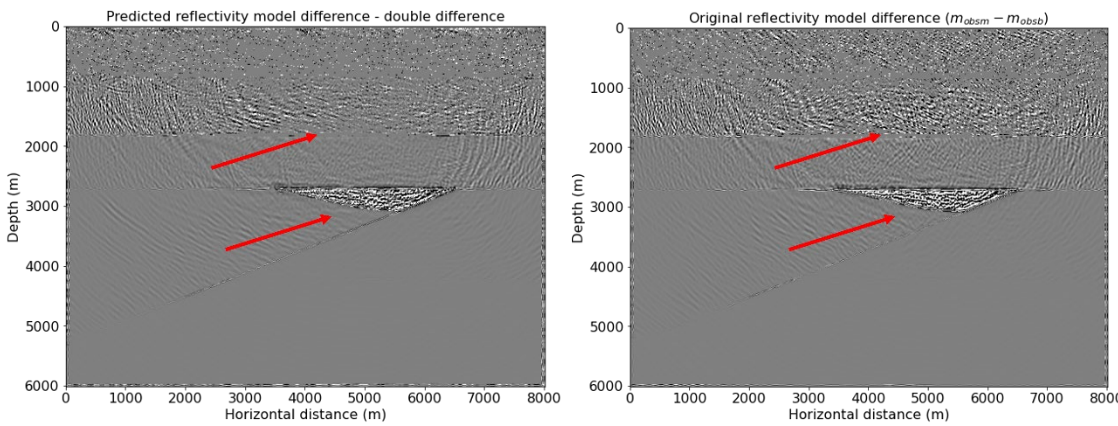

FIG. 1. Migrated result comparison between model difference from double-difference method (left), original model difference (right).

Comparing two basic approaches to decorrelation transforms

Kris Innanen, Marcelo Guarido, and Daniel Trad

ABSTRACT

Statistical decorrelation transforms map clusters of multivariate data to domains in which they are uncorrelated. In 2020 an algorithm was introduced to decorrelate deterministic optimization problems. In the approach, a given model space is re-parameterized such that a quadratic objective function defined on that space maps to one whose Hessian matrix is the unit; this procedure is immediately applicable to statistical decorrelation problems. The approach is essentially geometrical, in that involves designing the re-parameterization as a coordinate transform involving oblique-rectilinear basis vectors. In this paper the approach, which is procedurally very different from other decorrelation approaches, is investigated to understand what relationship it bears to standard methods, which are generally based on factorization algorithms. The results are suggestive that the geometric approach and its various realizations are different from existing methods, they may represent a generalization of the ZCA approach. The algorithm meanwhile may have some advantages, in that once one instance of the transform is constructed, alternate versions can be computed with little additional calculation.

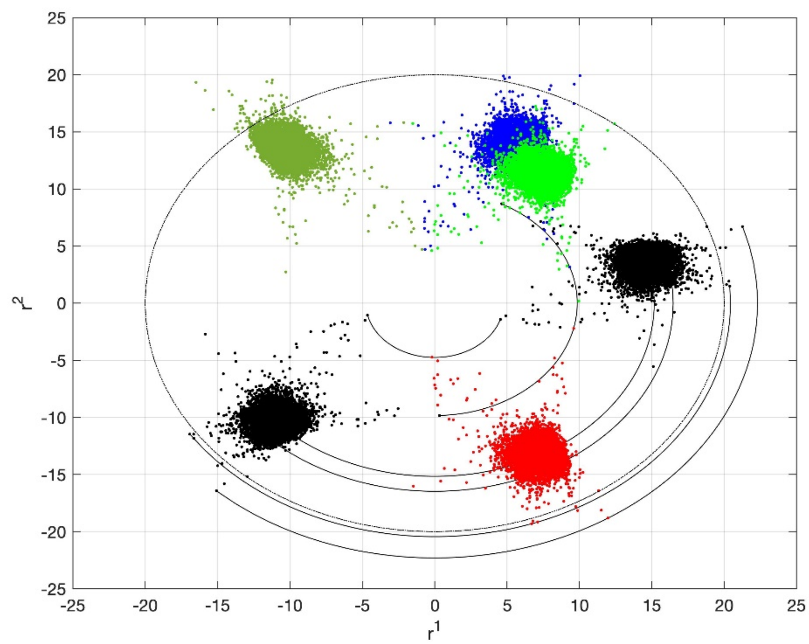

FIG. 1. A non-Gaussian, bivariate data cluster is subjected to several decorrelation transforms: ZCA (blue), PCA (khaki green), Cholesky (green), and a range of the direct/geometric approach (black/red). The general rotational relationship between all such transforms is visible, but we suggest that the range and attributes of the geometric approach make it practically quite different from standard approaches.

The linear algebra of entangled systems

Kris Innanen

ABSTRACT

The continuing (though gradual), development of applied geophysical algorithms and ideas in the area of quantum computing at CREWES, as well as our growing interest in characterizing inversion uncertainty with quasi-dynamical systems (inspired by the so-called Hamiltonian Monte Carlo methods), both motivate some review work on the linear algebra of quantum mechanics. The description of simple systems, in isolation and in combination, is developed, with the latter allowing simple entangled states to be discussed, which is relevant in quantum information and computing. *Laddering operators* in the description of harmonic oscillators are also given special focus: since in the above-mentioned Hamiltonian MC methods, energy and data misfit are associated, laddering operators may be useful descriptors of convergence. Steps needed to increase the dimensionality of systems, and steps needed to increase the number of particles/oscillators in systems are also given attention, since both will be needed in evolving applications in optimization and geophysical quantum computing.

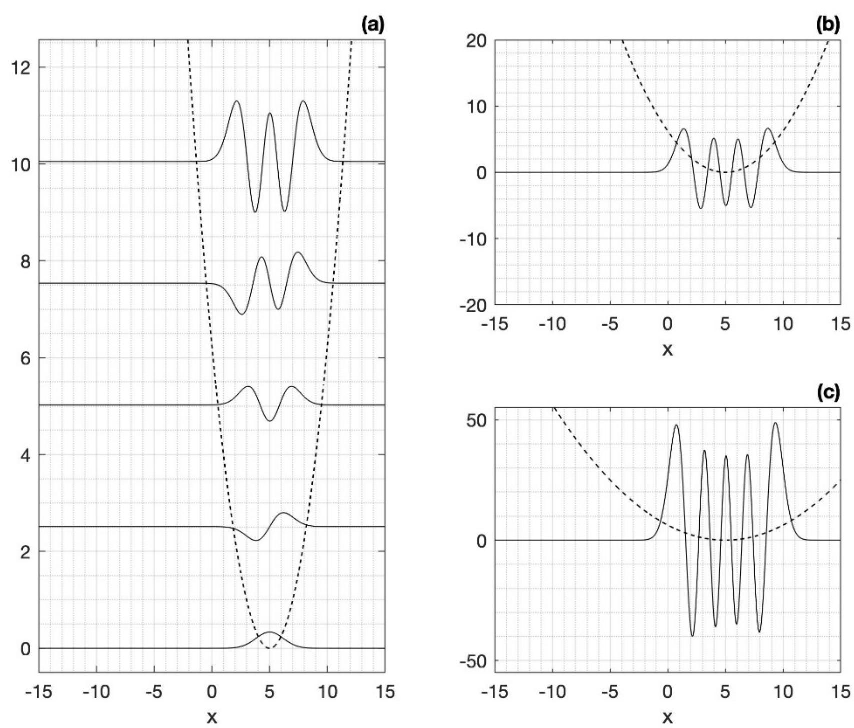

FIG. 1. (a) Ground and excited states of the 1D harmonic oscillator. (b)-(c) Higher energy excited states: probability of observing the particle away from equilibrium grows. Suppose the parabolic potential was a misfit function – can we characterize our state of knowledge of the model with such wave functions? Can we discuss convergence using the laddering operators which transition us from high to low energy?

A time-lapse multi-offset, multi-azimuth VSP acquired as a candidate for low-cost monitoring of CO_2 injection and storage

Kris Innanen*, Kevin W. Hall, and Don Lawton

ABSTRACT

In August 2022, CREWES returned to the field to carry out a monitoring version of the 2018 multi-offset/azimuth VSP survey referred to as the Snowflake. The purpose is to add to the datasets which enable research into CO$_2$ injection/storage monitoring (through, e.g., FWI methods), side-by-side comparisons of standard geophone and accelerometer sensors with both straight and helical wound fiber, and (now), enable research into methods for time lapse analysis, whether involving FWI or other methodologies. Partners Echo Seismic and HDSC worked with University of Calgary/CREWES researchers to acquire a data set designed to maximize repeatability while adding several new dimensions. For instance, two of the VSP azimuths were re-shot with low-dwell as opposed to linear sweeps. Observing differences in effectiveness in waveform and standard analysis methods between these two sweep types is expected to shed significant light on optimal monitoring. This globally unique dataset, coupled with its baseline 2018 counterpart, is expected to support years of groundbreaking research.

FIG. 1. Left: Echo Seismic INOVA AHV-4 vibroseis source, shooting into HDVSP accelerometer tool. Right: University of Calgary OptaSense ODH4 DAS interrogator.

Cross-gradient regularization for multiparameter FWI of physically modeled data

Scott Keating*, Kris Innanen, and Joe Wong

ABSTRACT

In 2022 an in-plane, surround acquisition ultrasonic survey was acquired in the physical modeling lab. Buzzer sources, operating at the low end of the ultrasonic spectrum were employed. These data were inverted using a variable density acoustic, frequency domain full waveform inversion. Results demonstrated relatively robust capability to characterize the longer wavelength features of target cross-sections. Shorter wavelength features were more difficult to recover. This effect is likely linked to the lack of complete reflection measurements in the data, which may have impeded accurate characterization of reflection behaviour. A cross-gradient regularization was able to enforce geometric similarity between the density and velocity models recovered by the inversion.

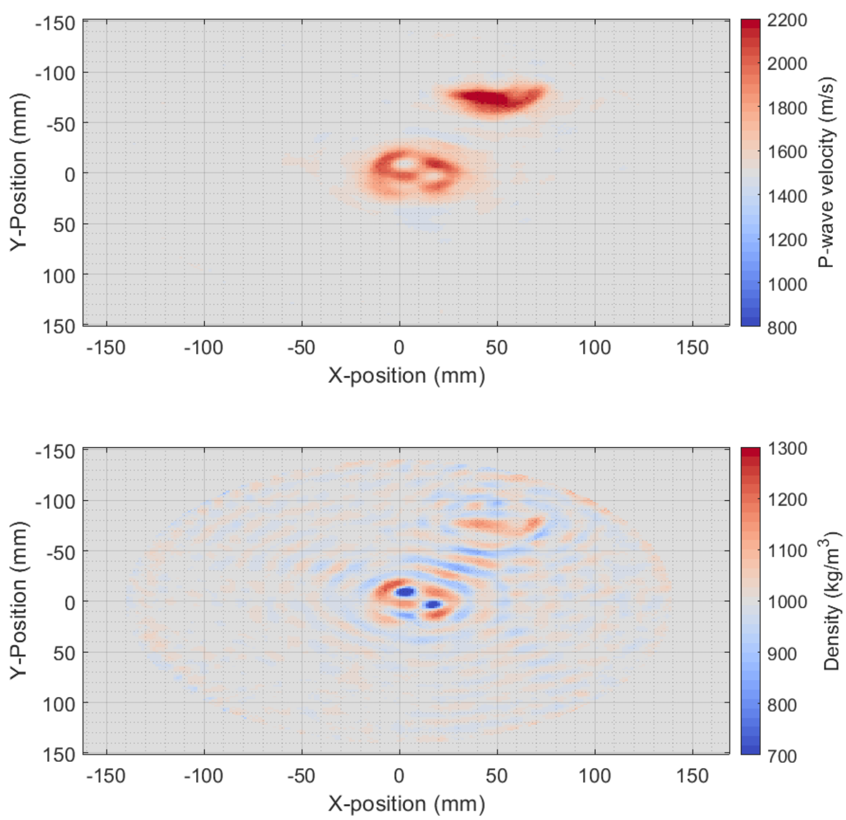

FIG. 1. Baseline inversion (top left), monitor inversion (top right), their difference (bottom left), and the shuttled difference (bottom right) for a synthetic time-lapse case with noise and inconsistent acquisition.

Preliminary FWI results from Snowflake II

Scott Keating* and Kris Innanen

ABSTRACT

In 2022 a vertical seismic profile survey was shot at the Carbon Management Canada Newell County Facility as a follow-up to a 2018 survey, after years of CO_2 injection at the site. We perform preliminary processing and inversion of the new data, using the inversion approaches and parameters used on the 2018 data set. Probable errors in the inversion output motivate a strong possibility that several of the inversion parameters may need to be modified to achieve a comparable result with the 2022 data set.

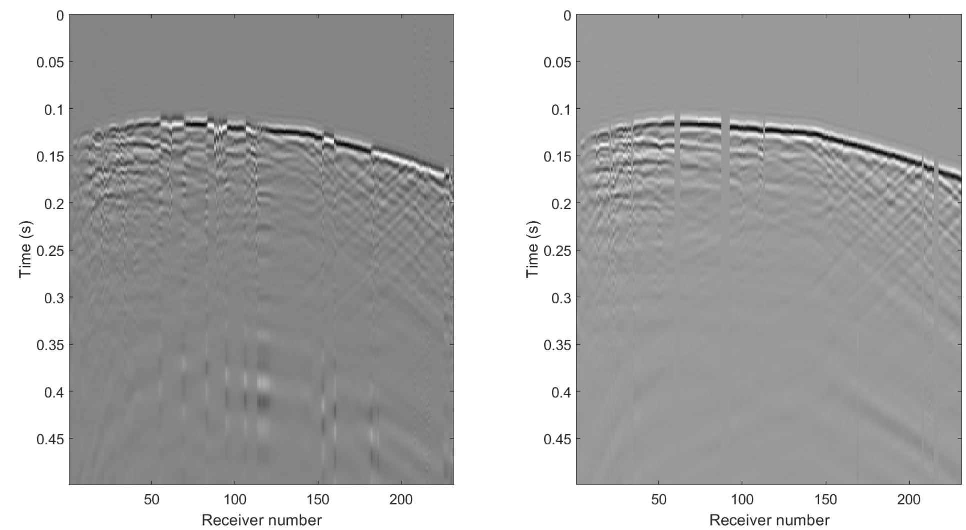

FIG. 1. Horizontal component before (left) and after (right) rotation and muting of bad traces for 220m offset shot.

Targeted nullspace shuttling in time-lapse FWI

Scott Keating* and Kris Innanen

ABSTRACT

Time lapse inversion plays an important role in monitoring applications. Conventional approaches rely primarily on differencing strategies in either data or model space. The results of the model difference based approaches can be strongly influenced by the choice of starting model for baseline and monitor inversions. Different choices can result in different levels of mitigation of non-reproducible survey effects (for instance noise). We propose an approach that substitutes the importance of the initial model choice with explicit navigation of the inversion nullspace. In this strategy, targeted nullspace shuttling is used to find the baseline and monitor models that minimize the difference between models while preserving a desired level of data-fitting. In synthetic examples, this approach demonstrates a significant capacity to mitigate the effects or non-reproducible noise and changing acquisition, and to identify when time-lapse differences fall below the confidence threshold described by nullspace shuttling.

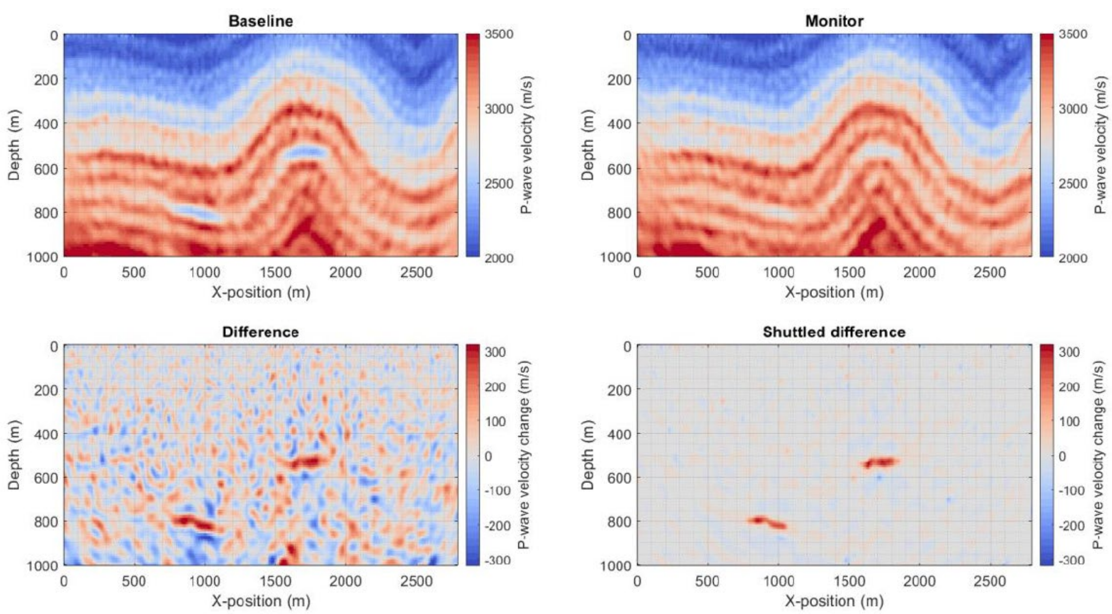

FIG. 1. Baseline inversion (top left), monitor inversion (top right), their difference (bottom left), and the shuttled difference (bottom right) for a synthetic time-lapse case with noise and inconsistent acquisition.

User guide for the CREWES frequency domain FWI codes

Scott Keating and Kris Innanen

ABSTRACT

Several of the projects reported on in this and previous research reports are based on a frequency-domain FWI code used by CREWES. This code is two dimensional, and forms using acoustic, elastic and viscoelastic wave propagation exist. The code is not suitable for 3D or large scale problems, but can be useful for analyzing the FWI problem through synthetic examples and relatively small field data sets.

In this report, we provide a user guide for the use of these frequency-domain codes. In this report, our focus is on the elastic implementation in the example code package "Elastic". This is planned to be the first of a set of user guides, which will be updated in the future. Please contact Kevin Hall in order to get the most recent version.

The report is organized into three main sections. The first section explains how to specify an inversion problem to the code and run it, the second section suggests some troubleshooting strategies for when errors are encountered, and the third section suggests where to modify the code for some common alterations.

Monitoring geological carbon storage: detection threshold at the CaMI Newell County Facility and a look ahead at a sparse monitoring approach for gigatonne scale storage

Don Lawton*[1,2], Brendan Kolkman-Quinn[1,2], and Marie Macquet[2]

ABSTRACT

Monitoring CO_2 injection at the CaMI Newell County Facility has continued with a broad range of monitoring technologies being implemented and evaluated. At the site, small volumes of CO_2 are being injected into a sandstone reservoir at 300 m depth, simulating a CO_2 leak from a deep geological carbon storage project. Time-lapse multi-offset and multi-azimuth vertical seismic profiles (VSP) and time-lapse electrical resistivity (ERT) surveys have both been successful at imaging less than 50 tonnes of CO_2 at this injection program. Figure 1 shows examples of VSP-CDP time-lapse seismic sections from one of the walk-away lines. Figures 1a and 1b are difference sections between the pre-injection baseline VSP data recorded in 2017 and monitor surveys recorded in 2021 and 2022 respectively. Figure 1c is the second-order difference between the data shown in Figures 1a and 1b, with the interpretation that CO_2 has migrated up-section in the storage complex between 2021 and 2022. ERT time-lapse results also support this interpretation.

For seismic monitoring of large-scale geologic carbon storage projects there are 4 main challenges - repeatability, resolution, how often we repeat the seismic surveys, and the cost of full-scale surveys that extend over the anticipated area of the CO_2 plume and/or pressure front. One monitoring approach that we are proposing is to use sparse nodes of sub-permanent seismic sources and permanent receivers that can be deployed on an expanding basis during the injection program as the plume develops. The separation of the source and receivers will be determined by an optimum offset to maximize the signal-to-noise ratio of the reflections from the CO_2 storage zone.

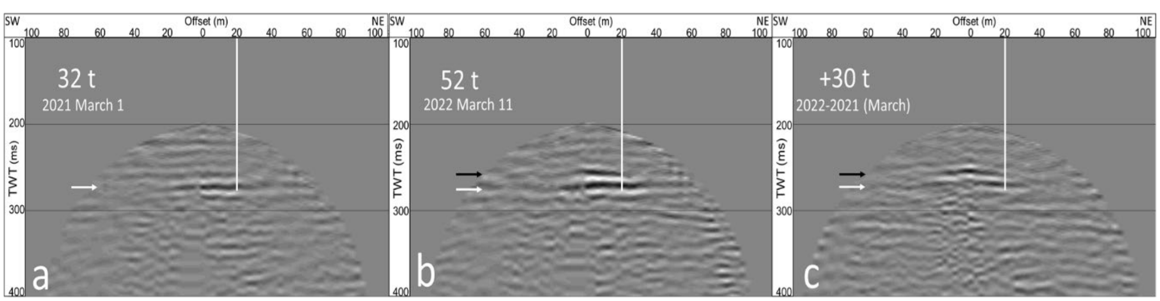

FIG. 1. Time-lapse VSP CDP difference sections from (a) 2021 and (b) 2022 and (c) the second-order difference between these.

[1] University of Calgary
[2] Carbon Management Canada

Robust reconstruction via Group Sparsity with Radon operators

Ji Li and Daniel Trad

ABSTRACT

Sparse solutions of linear systems play an important role in seismic data processing, including denoising and interpolation. An additional structure called group sparsity can be used to improve the performance of the sparse inversion. We propose a robust group sparse inversion algorithm based on Orthogonal Matching Pursuit with the Radon operators in the frequency slowness (w-p) domain. The proposed algorithm is used to interpolate seismic data and attenuate erratic noise simultaneously. During each iteration, The proposed algorithm first picks the dominant slowness group. Then, all the Radon coefficients located within the currently selected slowness groups are fit to the data in the time-space (t-x) domain via a robust solver, which is a $\ell 1-\ell 1$ ADMM solver. In other words, we adopt a cost function that directly utilizes the selected coefficients to fit synthesized signals via $\ell 1-\ell 1$ norm in the time-space domain. We prove that the proposed algorithm is resistant to erratic noise, making it attractive to applications such as simultaneous source deblending and reconstruction of noisy onshore datasets. We compare the performance of the same method with and without the group sparsity constraint and also with other Radon-based inversion methods. The result shows that the strong group sparsity inversion performs better than the traditional sparsity inversion. Both synthetic and real seismic data are being tested to examine the performance of the proposed algorithm.

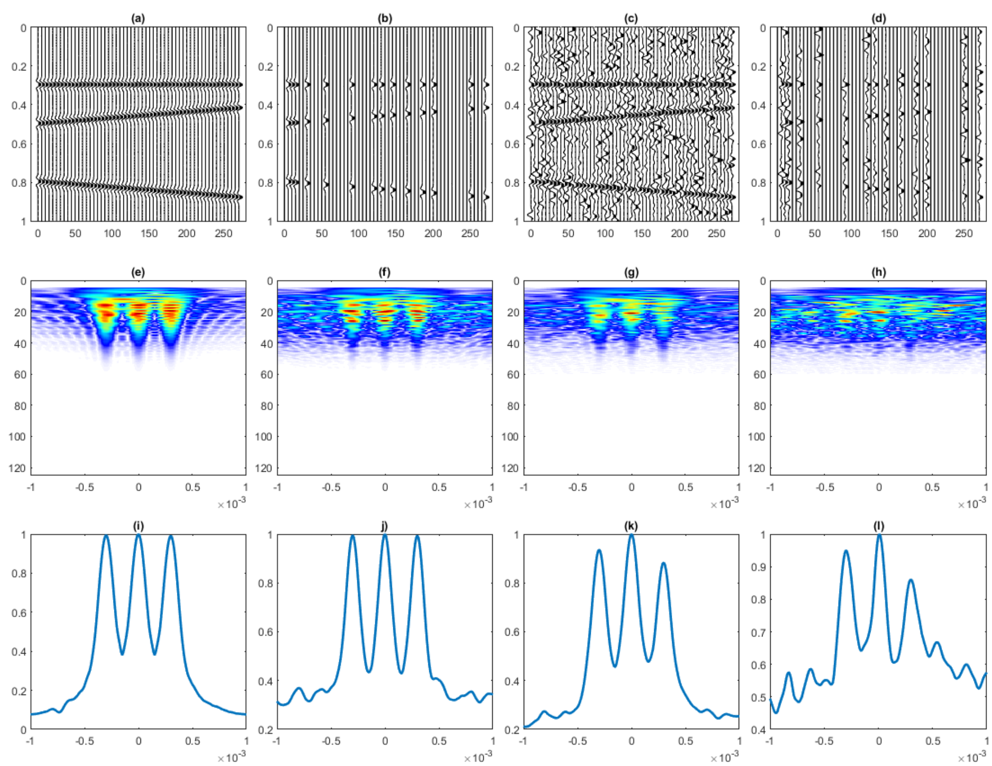

FIG. 1. (a)-(d): Clean data, data with missed traces, data with erratic noise, data with missed traces and erratic noise. (e)-(h): Corresponding f-p panel. (i)-(l): Corresponding norm map of the groups.

Instruction for C++ package of visco-elastic multiparameter FWI in the frequency domain

Jinji Li, Scott Keating, Daniel Trad, and Kris Innanen

ABSTRACT

The frequency domain full-waveform inversion (FWI) is a nonlinear optimization problem where large matrices such as the Helmholtz matrix and many derivatives are saved and utilized. In many inversion tests involving multiple variables and larger-scale models, the computational cost and consumption of computer resources should be considered. Matlab is presumably the best platform for solving large linear systems, manipulating matrices, and intuitively analyzing the intermediate results. However, its massive memory occupation and limited computational effectiveness can hamper going to 3-D problems or some larger 2-D FWI. Motivated by this, we developed a C++ version of the current 2-D frequency domain multi-parameter visco-elastic FWI, which can be carried out on relatively larger models. The reduced cost also allows us to go to the 3-dimensional inverse problems or the probabilistic approaches. Essential tools and concepts for working within the C++ ecosystem are covered in this instructive report, with examples of how to use this package.

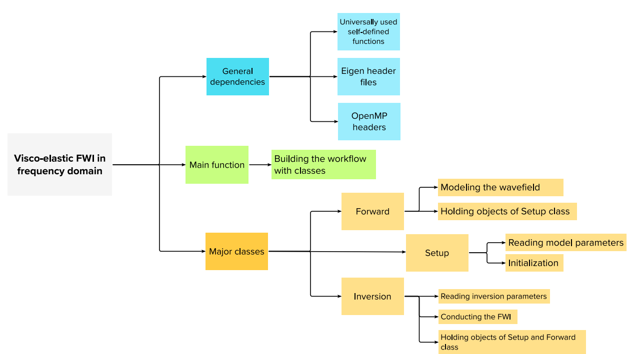

FIG. 1. Basic structure of VEFWI package.

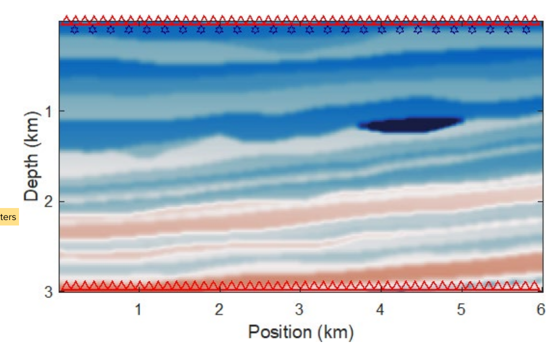

FIG. 2. Acquisition system in numerical test.

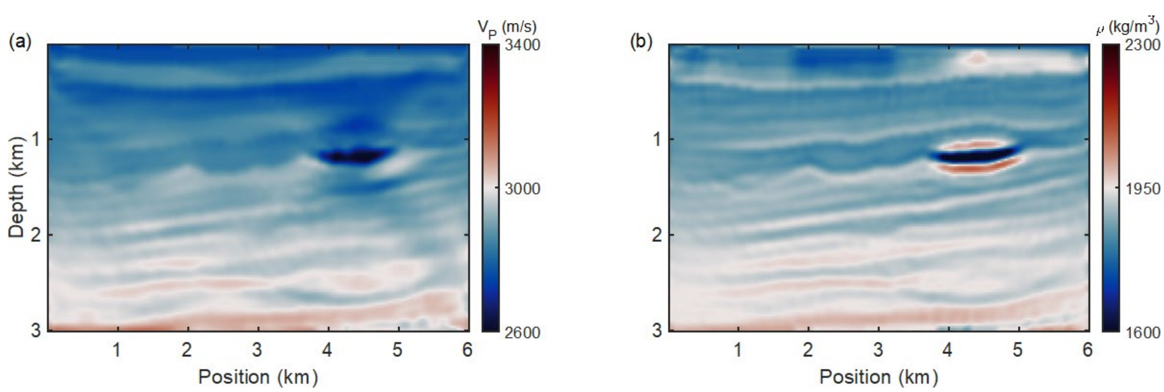

FIG. 3. Estimated models. (a) P-velocity. (b)density.

Simultaneous waveform inversion of SWD data for P-wave velocity, density, and source parameters

Jinji Li*, Scott Keating, Kris Innanen, and Roman Shor

ABSTRACT

Full-waveform inversion (FWI), as an optimization-based approach to estimating subsurface models, is limited by incomplete acquisition and illumination of the subsurface. Adding data corresponding to new and independent ray paths as input could significantly increase FWI models' reliability. In principle, seismic-while-drilling (SWD) technology can supply these additional ray paths; however, it introduces a new suite of unknowns, namely precise source locations (i.e., drilling path), source signature, and radiation characteristics. Here we formulate a new FWI algorithm in which source radiation patterns and positions join the velocity and density values of the grid cells as unknowns to be determined. We then conduct several numerical inversion experiments with the SWD sources located along a plausible well-trajectory with different source settings through a synthetic model. These SWD sources are supplemented by explosive sources and multicomponent receivers at the surface, simulating a conventional surface acquisition geometry. The subsurface model and SWD source properties are recovered and analyzed. After adding SWD data, both the inversion of physical elastic properties and source mechanisms get considerably enhanced, even in the cases where low frequencies are missing; the inversion also shows preferences on the features of the sequence of SWD sources along the trajectory. This model-source inversion algorithm also indicates the potential to simultaneously estimate the anelastic properties and trajectory deviation while drilling.

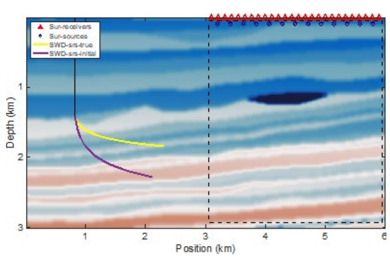

FIG. 1. True model and acquisition.

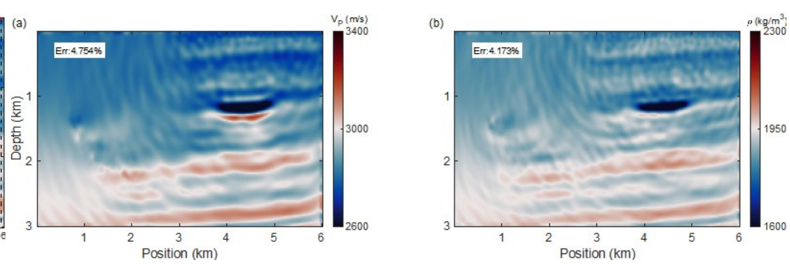

FIG. 2. Estimated models. (a) P-velocity. (b) density.

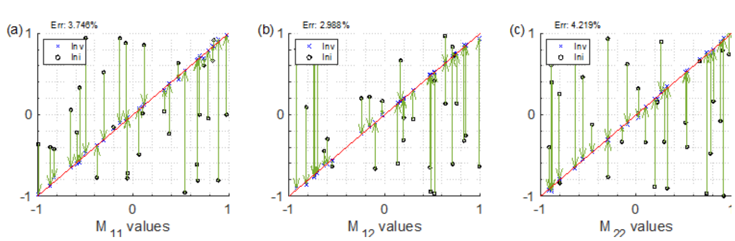

FIG. 3. Estimation of moment tensors. (a) M_{11}. (b) M_{12}. (c) M_{22}.

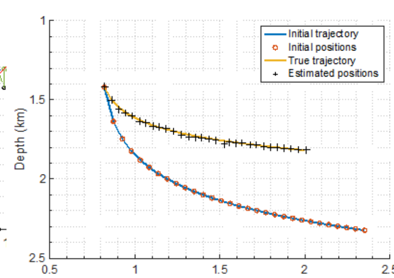

FIG. 4. Estimated trajectory.

Time-lapse FWI using simultaneous sources

He Liu*, Xin Fu, Daniel Trad, and Kris Innanen

ABSTRACT

Full waveform inversion (FWI) has been used to estimate high-resolution subsurface velocity models. It has become a powerful tool for time-lapse seismic inversion, which is promising to monitor reservoir profile changes with injection and production, and potentially long-term storage of CO2. To overcome the challenge of expensive computational costs for FWI process, shot subsampling methods and source-encoding strategies have been used to make the full waveform inversion efficient while maintaining the quality of the inversion results with minimum sacrifice. The cyclic method subsamples the shots at a regular interval and changes the shot subset at each iteration step. Using this method, we can suppress the aliasing noise present in regular-interval subsampling. FWI using source-encoding strategies has been investigated using different methods. In previous work, we have used an amplitude-encoding strategy with different bases to accelerate the FWI process. In this work, we incorporate amplitude-encoding strategy with cyclic subsampled data scheme, which first subsamples the data cyclically and then compose blended during the iterations. In this way, we can directly eliminate much more crosstalk terms introduced by encoded individual shot gathers and reduce the data dimension to improve FWI efficiency. We have applied this strategy to acoustic and elastic time-lapse FWI in time domain, and the synthetic inversion results recovered the velocity profile changes in the time-lapse models very well with reduced computation efforts.

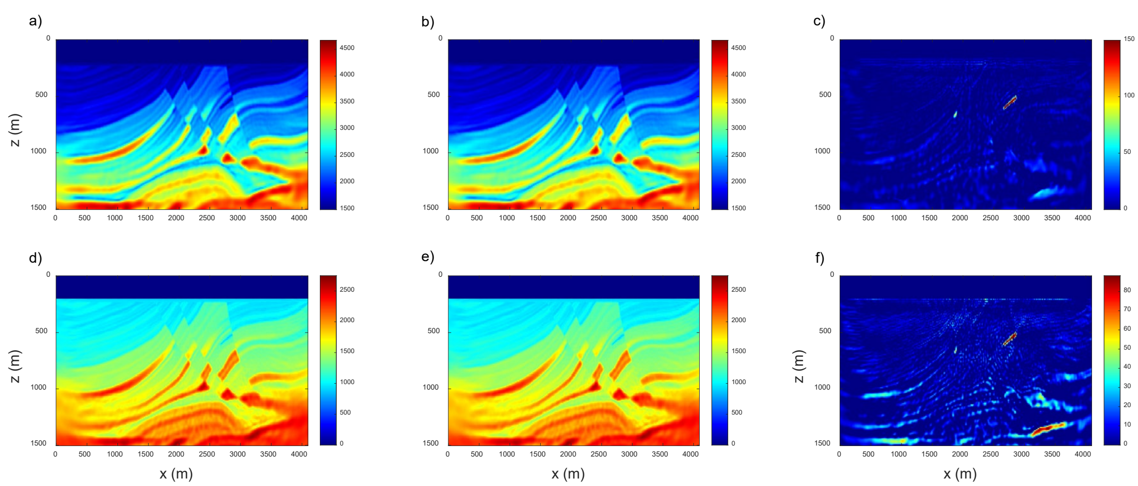

FIG. 1. Inversion results for elastic parameters: columns from left to right are the baseline, monitor and time-lapse vp and vs profiles.

Empirical radiation patterns as a method to assess crosstalk under scenarios of heterogeneous reference media

Mariana Lume, Ivan J. Sánchez-Galvis, and Kris Innanen

ABSTRACT

Analysis of radiation patterns is the most common method to evaluate crosstalk between parameters in Full Waveform Inversion problems. Typically, these are constructed from analytic expressions subject to not so realistic assumptions, such as the use of homogeneous reference media. This study focuses on introducing a workflow to extract the empirical radiation patterns from simulated scattered wavefields and on making use of it to assess the V_P, V_S and ρ scattering patterns generated from wavefields produced under different heterogeneous backgrounds. To achieve this, radius dependent masks to isolate displacements of interest and sweeps of angles were used. The proposed workflow is beneficial since it allows to extract highly accurate empirical patterns and demonstrates that, under heterogeneous scenarios, the shape of the radiation patterns has certain changes from what is theoretically expected, and that slightly different crosstalk regions from those indicated by the analytic expressions might occur, as well as sensitivity variations.

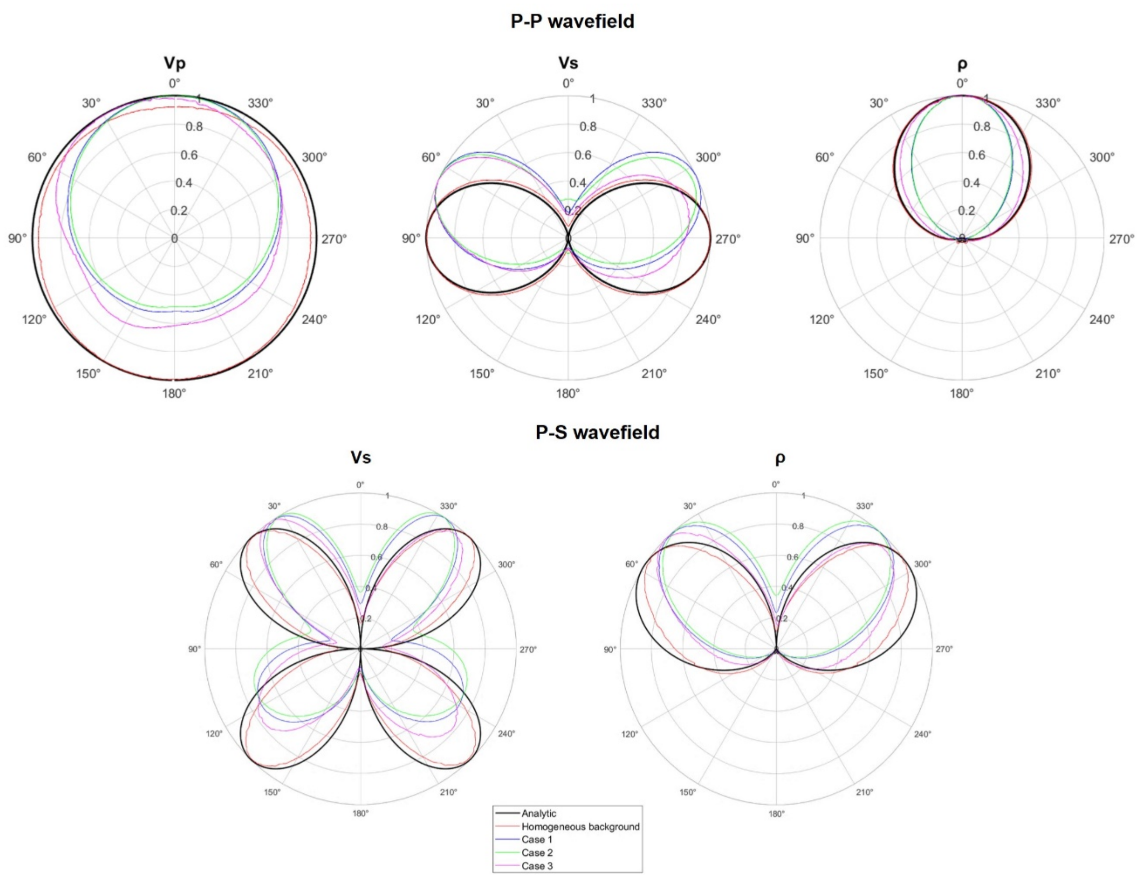

FIG. 1. Overlapped radiation patterns of analytic, homogeneous, and heterogeneous cases extracted from P-P and P-S wavefields.

Towards improving crosstalk suppression in multiparameter FWI by decorrelating parameter classes

Mariana Lume*, Scott Keating, and Kris Innanen

ABSTRACT

Multiparameter FWI is commonly affected by parameter crosstalk. These effects are described/corrected by the Hessian, which also impact the shape of the objective function iso-surfaces and the convergence of the optimization algorithms. This study focuses on finding an intermediate model space where the parameter classes are decorrelated, i.e., where the Hessian is an identity matrix, to minimize crosstalk and reach an accurate minimum that could be transformed to the ρ, V_P and V_S model space. Transformation rules between model spaces were applied in a FWI workflow, using transformation matrices (**T**) constructed to satisfy constraints imposed by the Hessian of the intermediate system. Overall, this FWI method produced relatively good V_S estimations, but did not overcome a reference FWI in the V_P and ρ results, since more crosstalk was introduced. However, improvements on the structure of the Hessians with respect to those from the reference inversion were brought for some areas of the model grid, which makes the main decorrelation ideas promising to minimize these coupled effects. The drawbacks were related to a localized approach to compute **T**, which might need to account, in future work, for crosstalk contributions of multiple grid cells.

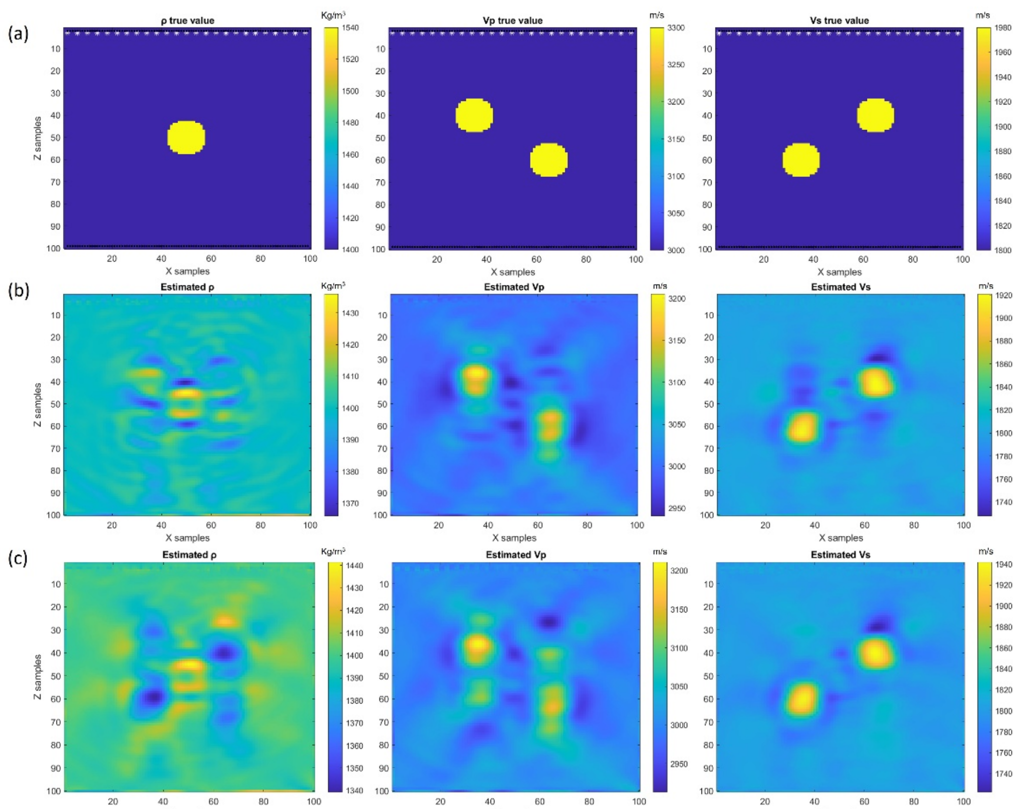

FIG. 1. (a) True V_P, V_S, ρ models and models estimated from (b) a baseline FWI and (c) a re-parameterized FWI after selecting location x=50 and z=20 to compute **T**.

Rock Facies Imbalanced Classification with Over-Sampling Techniques

Ryan A. Mardani and Daniel Trad

ABSTRACT

In classification problems, if the dataset is skewed, most machine learning algorithms produce poor prediction results for minor classes. In this study, we used different over-sampling techniques to balance the dataset that includes well logs and rock facies. XGBoost model is employed for this multi-class classification problem. We found that oversampling can improve prediction results in minor classes. Overall, Synthetic Minority Oversampling Technique (SMOTE) is a better candidate for oversampling, though for some classes Adaptive Synthetic Sampling (ADASYN) could compete with the SMOTE performance.

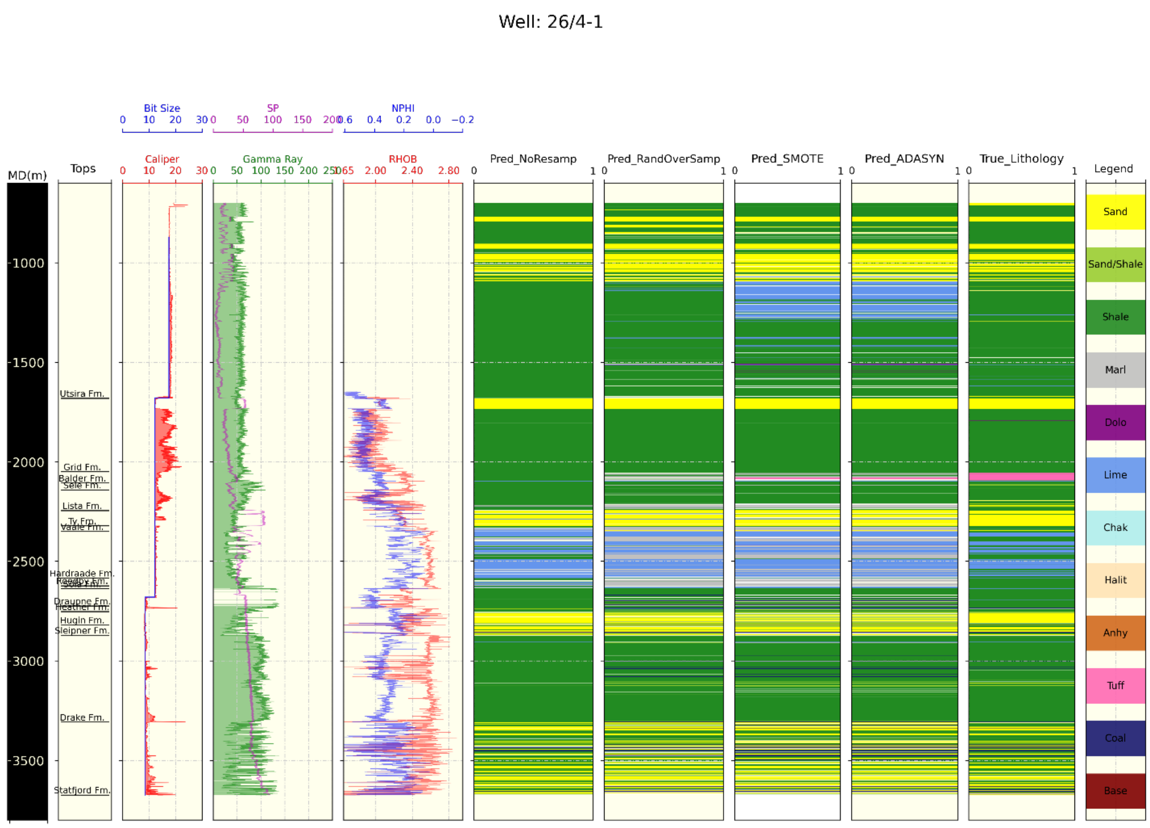

FIG. 1. plot of some well logs (predictors) and interpreted facies using various resampling methods along with actual lithology.

A quantum algorithm for traveltime tomography

Jorge E. Monsegny*, Daniel Trad, and Don Lawton

ABSTRACT

Quantum computation is described as a promising paradigm for the future. One of their advantages is the quantum parallelism, that consists in solving many instances of the same problem in a single run. This can be done due to the possibility to set a quantum system in a superposition of states. Although its main limitation is that only one of the states can be read at the end, it is possible to increase the chances of the state we are looking for. In this report we show a framework to pose the traveltime tomography problem, usually solved using gradient methods, as a quantum computing algorithm. This algorithm does a global exploration of the model space using the quantum parallelism. Then it manipulates the quantum phase of their states to increase the chances of reading the model that produces the global minimum. In that way we can read the tomography answer at the end of the quantum computation. Something important to notice is that there is no need to compute gradients or Hessians but only to do forward modelling and residual calculation. In this report we introduce only the notions needed to solve the inverse problem and we show a small example step by step to illustrate how the quantum algorithm works. The algorithm has been coded and run in a quantum simulator.

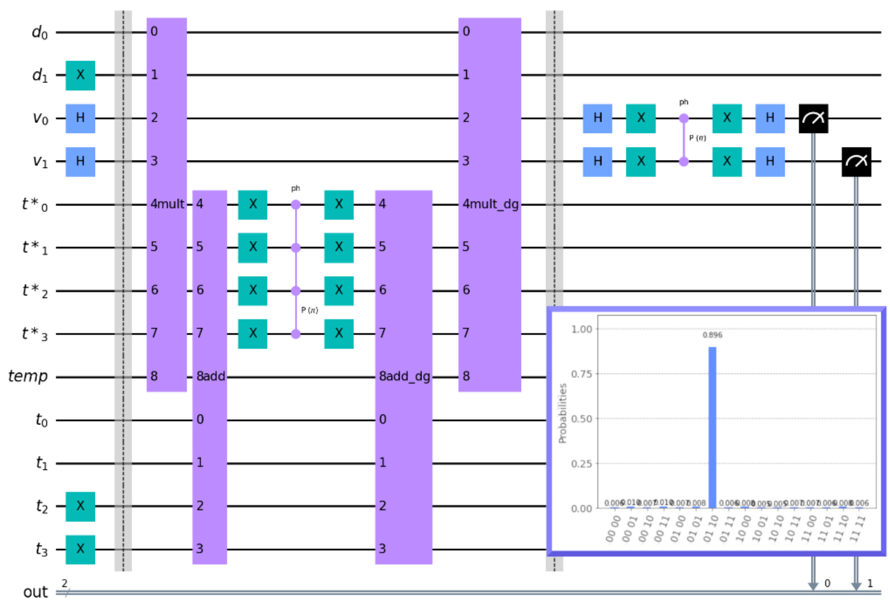

FIG. 1. Quantum traveltime tomography circuit. Horizontal lines are the qubits and bits. Quantum register $d = [d_1, d_0]$ has the raypath distances. Register $v = [v_1, v_0]$ contains the velocity models in superposition. Register $t^* = [t^*_3 - t^*_0]$ will have the calculated traveltimes. Register $t = [t_3 - t_0]$ has the measured traveltimes. There is one temporary qubit temp and two classical bits out where the output velocity model will be read to. The setup stage sets the input data and velocity models superposition. The Computation stage calculates the traveltimes and residuals, then it reverses the phase of the velocity model with zero residual. The mirror stage implements the quantum phase amplification circuit. At the end, a velocity model is read into the classical bits *out*. The insert on the right shows the simulation results where the inverted model has the highest probability.

A 2D full-waveform inversion using trench-deployed surfaceand VSP DAS data from CaMI.FRS

Luping Qu, Wenyong Pan, and Kris Innanen

ABSTRACT

A full-waveform inversion using trench-deployed surface waves and two wells' Vertical Seismic Profiling (VSP) data was conducted to generate a high-resolution S- and P-wave velocity models of the near surface at Containment and Monitoring Institute Field Research Station in Alberta. In this preliminary inversion, a sequential inversion was conducted by firstly inverting Vs using surface-wave FWI, and secondly inverting Vp using the VSP FWI. There are two datasets collected in August 2022 for the main CO2 monitoring line, line 13. They possess the same frequency range, with linear and low-dwell sweep, respectively. In this study, we compared these two datasets in detail. The inversion results are from the DAS data generated using the low-dwell sweep. Optical transport method was adopted to mitigate the cycle skipping problem mainly in surface wave inversion.

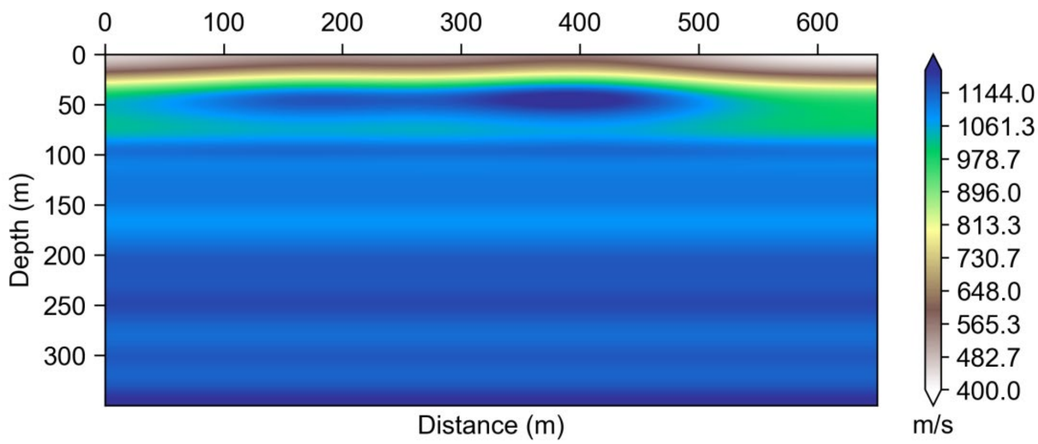

FIG. 1. The inverted Vs model of surface-wave FWI.

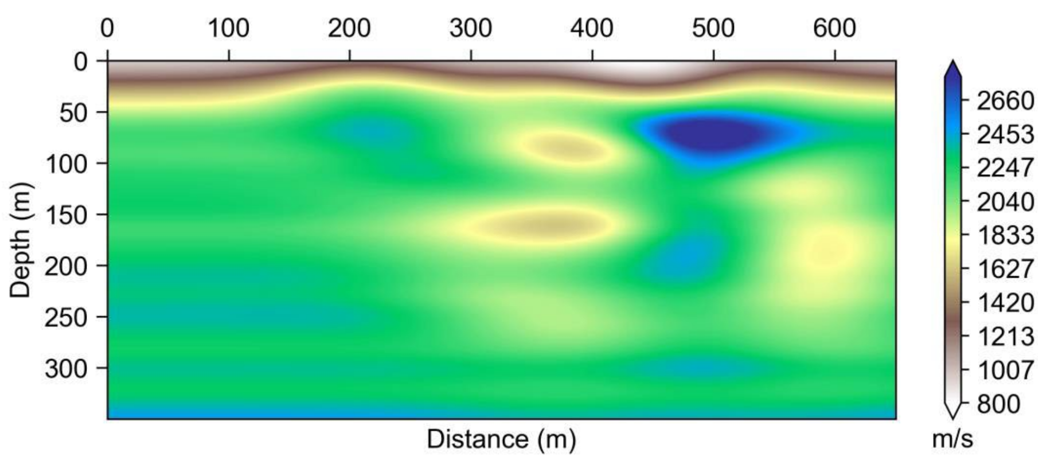

FIG. 2. The inverted Vp model of VSP FWI.

Incorporating estimates of data covariance in FWI to combat coherent noise based on auto-regressive process

Luping Qu*, Scott Keating, Xin Fu, He Liu, and Kris Innanen

ABSTRACT

An important step in seismic data processing is noise attenuation, which typically improves the subsurface seismic image and signal-to-noise ratio (SNR). In seismic records, coherent noise, which correlates spatially or temporally, are more difficult to attenuate or process as it can interfere with signals and be mistakenly recognized as signals. Through incorporating data covariance matrix into the misfit function, both the model parameters and noise can be estimated. When implementing this, the data covariance matrix with random noise can be simplified to be a vector. However, the data covariance matrix with coherent noise still need to be completely computed and stored. We find the serial data-error correlations can be characterized by adding the forward model with a autoregressive error model. As autoregressive error models do not estimate error with point estimates, the inverse of data-error covariance matrix does not need to be computed. The order of the autoregressive process required to fit the data is determined by the residual data-fitting examination. To avoid overfitting, estimates with several different orders were conducted and adopted in the following rounds of FWI.

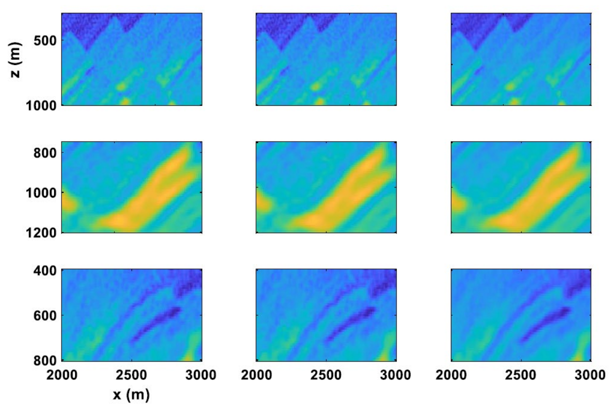

FIG 1. Inversion results. The left column are the inversion results using conventional misfit function, the middle column are the inversion results using generalized misfit function with AR model order equals 2, the right column are the inversion results using generalized misfit function with AR model order equals 3.

Poroelastic modeling of soap hole formation

Sarah Reid and Rachel Lauer

ABSTRACT

Soap holes were first identified >50 years ago as areas of localized surface weakness characterized by a thin and fragile crust covering sand, silt, clay, and water. It was hypothesized that they form where groundwater is moving upward to the ground surface through unconsolidated sediment. Soap holes are ubiquitous across the prairies and manifest as either mounds or flat exteriors underlain by liquefied mud. They range in diameter from less than 1-m to several meters and can reach up to several meters in depth. Due to their thin and fragile crust, they pose a risk to farming equipment and livestock, with several farmers reporting loss of cattle and extensive portions of land that are no longer farmable. Previous work has provided hydrological and geochemical constraints to create a conceptual model for soap hole formation. In this conceptual model, pressurized water from a confined aquifer travels upward through preferential flow paths in glacial till to a lacustrine deposit at the ground surface. There, the combined effects of increased fluid pressure and clay dispersion cause the soil to liquefy and form a soap hole. This study tests the conceptual model for soap hole formation by determining which parameters and processes impact the extent and volume of liquefaction in a 3-dimensional model using a steady state solution in COMSOL Multiphysics. In COMSOL, we employ Darcy's Law, solid mechanics, and poroelasticity to successfully approximate a simplified version of the observed field data. Variations in hydraulic, elastic, and geometric parameters were explored to determine their impact on the volume of liquefaction in the model. The results provide insight into the conditions required for soap hole formation, and serve to verify the conceptual model developed through field studies.

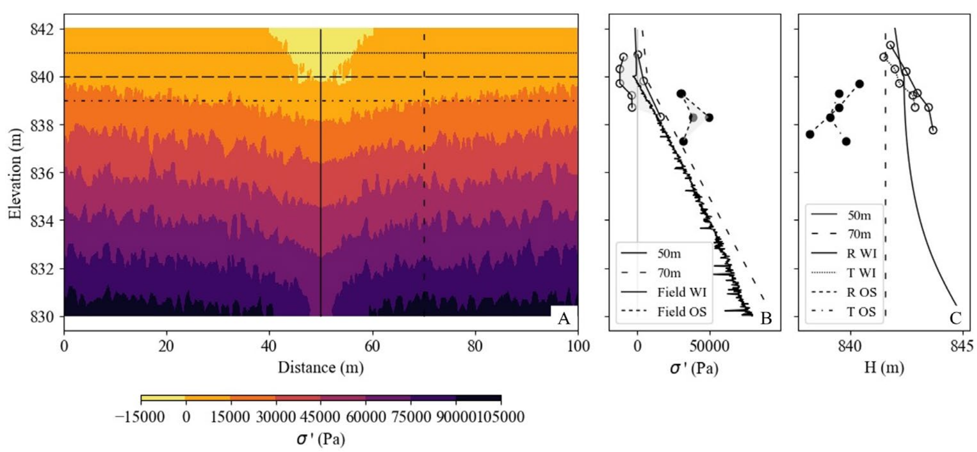

FIG. 1. The base model results. A) A vertical cross section taken at y = 50 m. The contours are for effective stress, where purple is high effective stress and yellow is low effective stress. An effective stress less than or equal to zero represents an area of liquefaction. B) Cut lines at 50 m and 70 m along the cross section are compared to field effective stress within (WI) and outside (OS) the soap holes at the field sites. C) The hydraulic conductivity in the model for the same cut lines are compared to the Rumsey (R) and Torrington (T) field sites.

The dual representation and its application to seismic reservoir analysis

Brian Russell*[1]

ABSTRACT

Geophysical and machine learning algorithms are based on finding the best weights that predict a set of observations from a set of measured features or attributes. A good example of this is the prediction of seismic reservoir parameters, such as density or porosity, from a set of seismic attributes. Many problems can be written as a linear regression model in which the weights can be determined using a generalized inverse. Although this involves a linearly weighted combination of the input attributes, we can apply a nonlinear function to the attributes themselves, which allows us to get a much better fit on the output. In this study I will consider two different forms of the generalized inverse, the primal and dual, and show the dual form leads to several very powerful analysis techniques, called kernel regression methods, that give much better fits than the multi-linear regression techniques used in many applications. I will illustrate these techniques using two simple datasets, one with only three points and the other with ten points, and then apply them to seismic reservoir analysis. The figure below shows that application of several machine learning algorithms to a dataset from Blackfoot, Alberta.

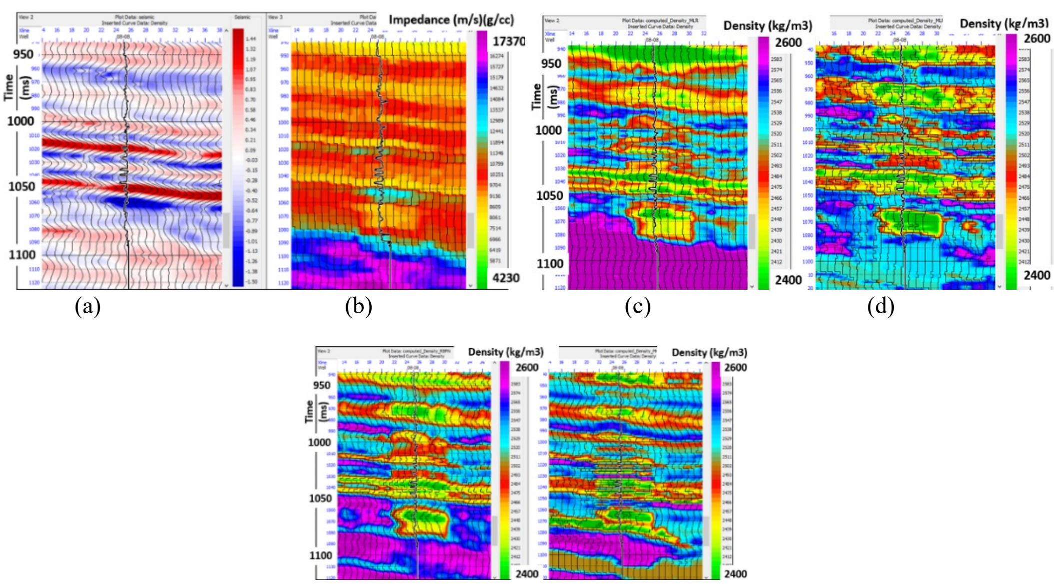

FIG 1. The results of applying machine learning algorithms to the prediction of density from seismic attributes, where (a) shows the seismic amplitudes, (b) shows inverted seismic impedance, (c) shows the multi-linear regression prediction of density, (d) shows the backpropagation neural network prediction of density, (e) shows the radial-basis function neural network prediction of density, and (f) shows the generalized regression neural network prediction of density, all on the same vertical cross-section from a 3D seismic volume.

[1] GeoSoftware, Calgary, Alberta

Attenuation surface noise with autoencoders

Ivan J. Sánchez-Galvis, Daniel Trad, William Agudelo, and Daniel Sierra.

ABSTRACT

Surface wave attenuation is one of the essential stages in data processing for land seismic exploration. Conventionally, this stage involves F-K filters that can separate the surface waves in a specific area of frequency and wavenumber domain. However, these filters must be tuned manually shot by shot according to the surface wave behavior in the acquisition zone. Thus the quality of the filtered data depends on human expertise, and processing times increase according to the number of shots. Moreover, the F-K filter requires seismic data with uniform spatial sampling, which is not possible in some complex land area acquisitions. Therefore, we propose to use a convolutional autoencoder to predict the Radon model of seismic data without surface wave noise. The Radon model allows working with seismic data with irregular spatial sampling. We train the autoencoder with synthetic data generated by elastic wave modeling with several 2D earth models. The results show that the trained model can accurately attenuate the surface noise with a performance similar to well-tuned F-K filters.

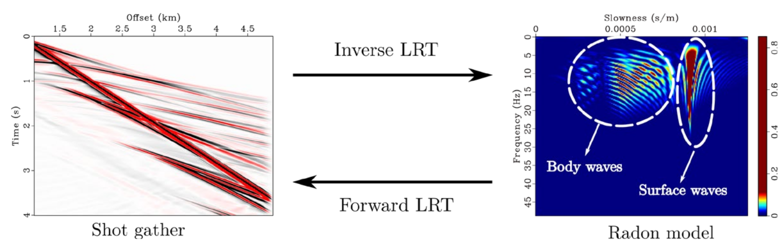

FIG 1. Aplication of the frequency domain Linear Radon Transform (LRT) on seismic data. The inverse LRT is used to estimate the Radon model (right) from the shot gather (left).

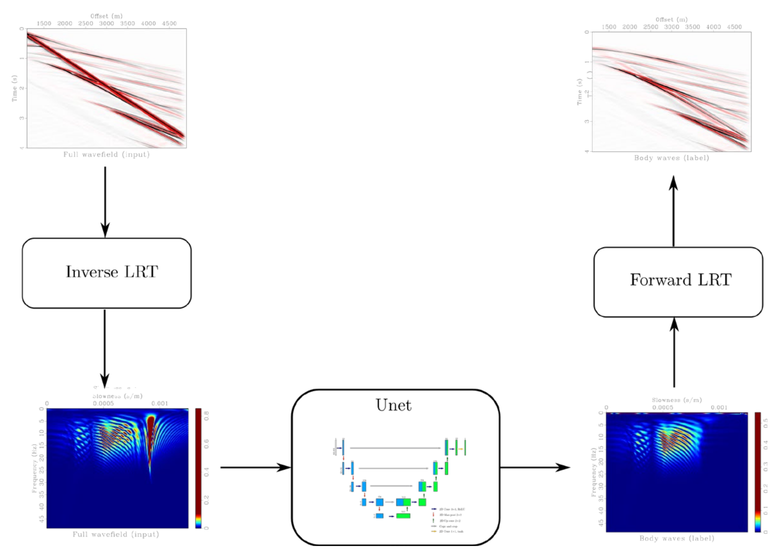

FIG. 2. Workflow to attenuate the surface wave noise in seismic data. The Radon model of the raw shot gather is the input of the Unet model. The output is the Radon model containing just the body wave information.

Polarization filter based on linear Radon transform and elliptical elements to extract surface waves in 3C seismic data

Ivan J. Sánchez-Galvis, William Agudelo, Daniel Trad, and Daniel Sierra

ABSTRACT

Polarization filters are an alternative tool to attenuate ground roll when multicomponent seismic data are available. These filters can separate surface and body waves by discriminating elliptical from linear motions. Existing polarization filters work in single-station. Thus, they can filter seismic data with irregular spatial sampling. However, in most cases, polarization filters do not get results similar to F-K filters because they do not operate in multitrace, and there is no velocity discrimination. We present a new polarization filter to extract surface waves from multitrace 3C seismic data. The filter works in the frequency-slowness domain as a mask on elliptic elements obtained from the linear Radon model of the seismic data in the frequency domain. We applied this filter on a 3C real shot gather from land seismic data acquired in the Middle Magdalena Valley in Colombia. The results show that this polarization filter can accurately extract the surface waves, preserving more low-frequency energy than the F-K filter.

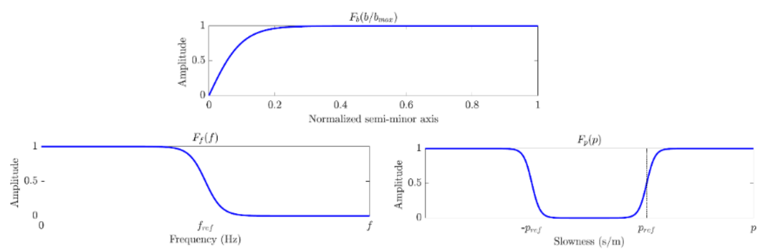

FIG. 3. Activation functions used to construct the polarization filter mask.

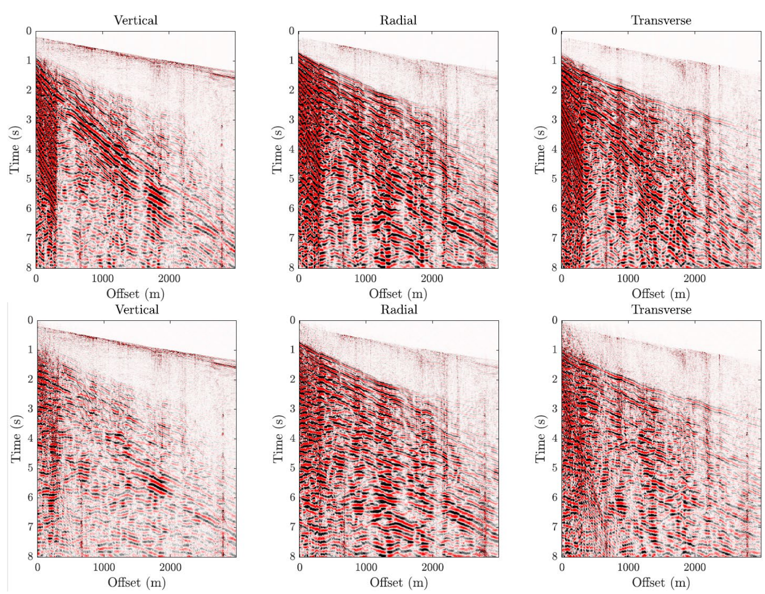

FIG. 4. Multicomponent shot gather of (top) raw data, (bottom) filtered data with the polarization filter

Common image gathers from blended data

Ziguang Su* and Daniel Trad

ABSTRACT

Common-image gathers, or CIGs, are essential for migration-based velocity analysis and amplitude-versus-angle analysis, which could be utilized to predict lithology, fluid properties, and create velocity models. Blended acquisition, also known as simultaneous seismic source acquisition, is a useful technique for boosting acquisition efficiency and improving the quality of the subsurface image. We offer a technique that uses reverse time migration based on direction vectors to calculate angle-domain common-image gathers (ADCIGs) straight from blended data. Our technique generates amplitude-preserved ADCIGs and takes into account subsurface folds in the image condition. Examples that contrast our method with exact Zoeppritz equations demonstrate its correctness. Our strategy also allows for the loosing of the acquisition restrictions of random source timings and placements.

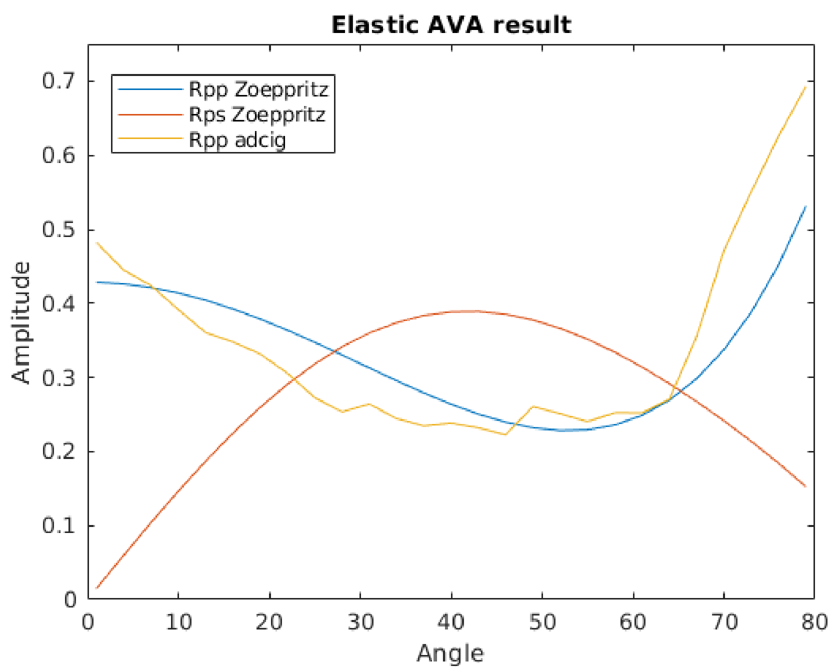

FIG. 1. Reflected PP wave Amplitude-versus-Angle response from exact Zoeppritz equation and ADCIG, and Reflected PS wave from exact Zoeppritz equation

Machine learning applications for seismic processing

Daniel Trad*

ABSTRACT

Machine learning (ML) is a powerful tool that has become very useful in many areas of science and seismic applications are not an exception. For example, the uses of ML in interpretation have proven to be very helpful. Also, in seismic processing, we see a significant effort for using ML techniques to help or replace traditional processing. Processing applications, however, present a more difficult challenge. In this report, we will discuss what some of those challenges are, and also we will discuss an environment to research this type of technique, where ML does not replace but rather cooperates with traditional signal processing and inversion. We will present this methodology with several examples: migration, multiple attenuation with Radon transform, near-surface noise (ground roll) suppression and interpolation. For the purpose of illustrating the flexibility of machine learning and the importance of data preprocessing, we will address all these problems by using the same deep learning network but changing only inputs and outputs. The goal of the report will be to emphasize the importance of combining conventional and neural network techniques.

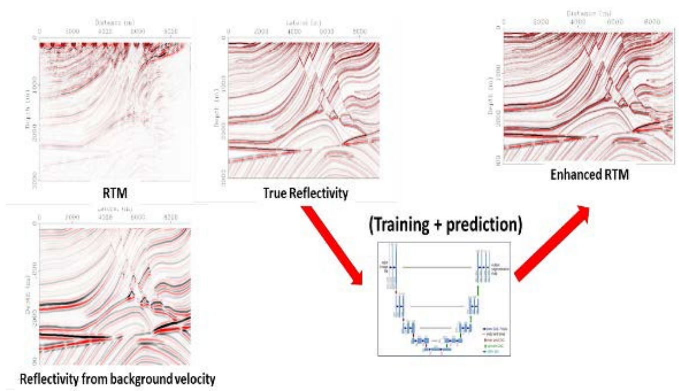

FIG. 1. Training using true reflectivity as label.

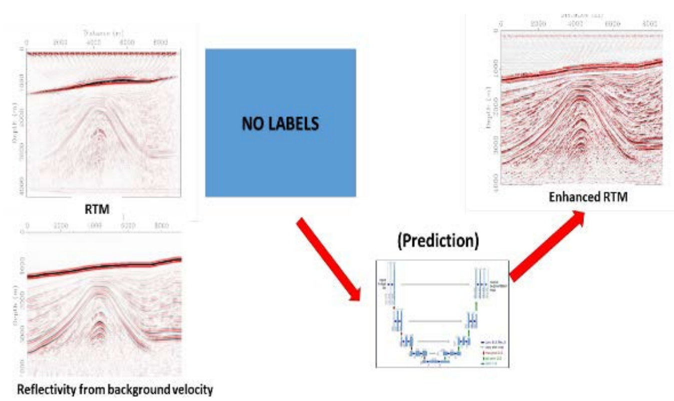

FIG. 2. Prediction with unknonw reflectivity.

Enhanced reverse time migration of walkaway VSP data

Jing Wang and Kris Innanen

ABSTRACT

Elastic reverse time migration is a vector wave theory-based depth domain migration algorithm. Wavefields separation is a key step to remove crosstalk artifacts and improve the imaging quality. This operation allows us to produce vector P- and S-wavefields with the same phases and amplitudes as the input coupled wavefields, while significantly reducing computational costs. The test results illustrate that the amplitude and phase of the separated wavefields are changed and the polarity is reversed after the Helmholtz decomposition, so that further correction are needed. Aiming to solve these problems, decoupled elastic wave equations are utilized to simulate the wavefields propagation, which can maintain the vector property of original wavefields without polarity reversal. With the separated vector wavefields, we implement a modified dot-product imaging condition for elastic reverse time migration, which produces migrated images with accurate amplitudes. Several numerical examples are used to demonstrate its feasibility and robustness for imaging complex subsurface structures. In this report, we firstly review the Helmholtz decomposition and analyze its shortcomings. Next, we utilize the decoupled elastic wave equations to obtain vector P- and S-wavefields with the same phases and amplitudes as the input coupled wavefields. And then, a dot-product imaging condition and corresponding elastic reverse time migration workflow are presented to produce PP- and PS-images. Finally, several numerical examples are used to illustrate the performance of this wavefield decomposition strategy and the corresponding workflow. Besides, the numerical simulation methods for the forward and backward wavefields' extrapolation, the effects of multiple waves are also discussed in this report to further improve the imaging efficiency and accuracy.

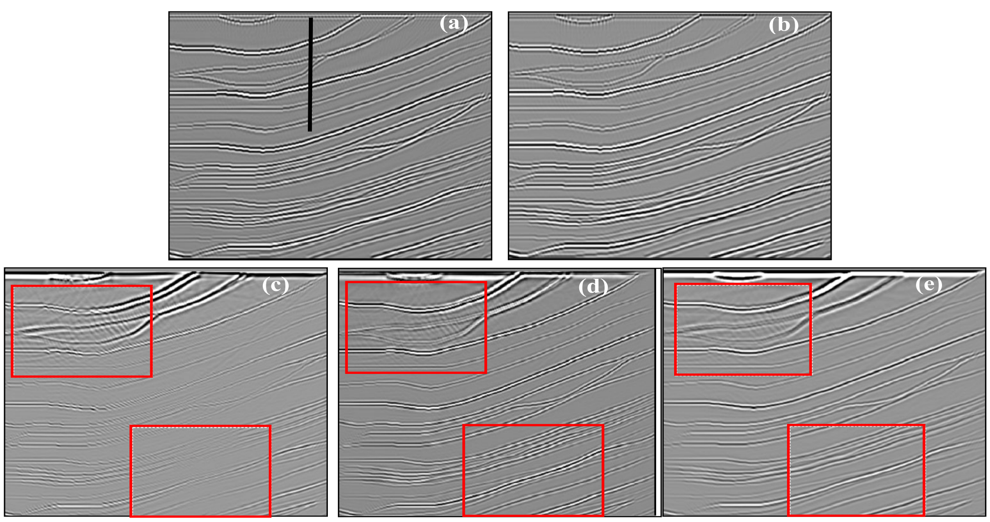

FIG. 1. Test imaging quality of the Marmousi truncation model. (a) PP imaging with Helmholtz decomposition, (b) PP imaging with decoupled elastic wave equation, (c) PS imaging with Helmholtz decomposition, (d) PS imaging with polarity correction-based Helmholtz decomposition, d) PS imaging with decoupled elastic wave equation.

Acoustic and exact elastic impedance variations during CO_2 injection at the CaMI.FRS

Yichuan Wang and Don Lawton

ABSTRACT

For seismic monitoring injected CO_2 during geologic CO_2 storage, it is useful to measure time-lapse (TL) variations of seismic impedance. Acoustic impedance (AI) and elastic impedance (EI) give direct connections to the mechanical and fluid-related properties of the CO_2 storage complex. However, evaluation of their subtle TL variations is complicated by the scaling and low-frequency uncertainties, and the various EI definitions involve different approximations and do not represent an elastic property of the medium. To solve these issues, we perform accurate waveform calibration for TL seismic data, and apply a robust impedance-inversion approach based on calibration of seismic records by using the well-log data. We also use an exact expression of EI in a matrix form, which truly represents the intrinsic physical property and accurately describes P- and S-wave propagations at arbitrary incidence angles. The above approaches are applied to TL DAS VSP data from the Field Research Station CO_2 injection project in southern Alberta, Canada. High-quality baseline, monitor and TL impedance-difference images are obtained. TL impedance variations are observed within the CO_2 injection zone, which are interpreted as being related to the CO_2 injection. AI and EI measured from this approach can be advantageous tools for monitoring the distribution and migration of CO_2 plumes within the CO_2 storage complex.

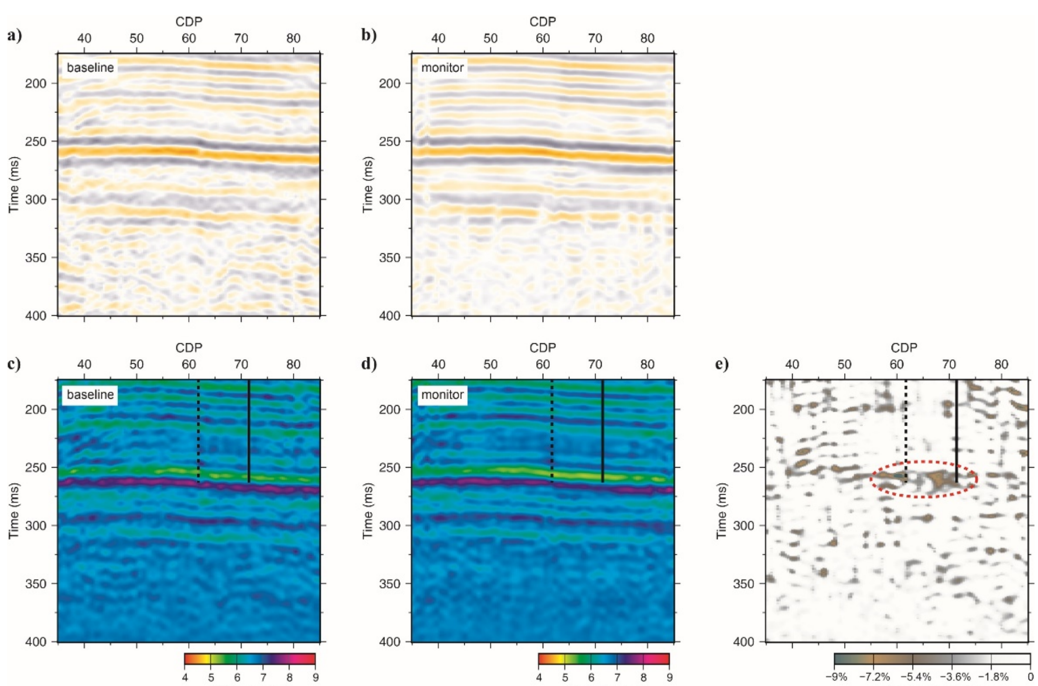

FIG. 5. Cross sections of AI and their relative variations along Line 13: (a and b) baseline and monitor VSP CDP stack and the corresponding (c and d) baseline and monitor AI derived by our inversion approach, and (e) relative AI variations between (c) and (d). Dashed and solid black lines indicate observation well and injection well, respectively.

Time-lapse attenuation-attribute variations during CO_2 injection using DAS VSP data from the CaMI.FRS

Yichuan Wang* and Don Lawton

ABSTRACT

For seismic monitoring injected CO_2 during geologic CO_2 storage, it is useful to measure time-lapse (TL) variations of seismic attenuation. Seismic attenuation directly connects to different petrophysical parameters of the CO_2 storage complex. We have developed an approach to derive smooth time-variant spectra from seismic signal by using sparse strongest signal peaks, and then measure two different attributes characterizing the path effects of seismic attenuation from the smooth spectra. This approach is straightforward and does not require sophisticated algorithm or parameterization scheme. We apply this approach to TL DAS VSP data from the Field Research Station (FRS) CO_2 injection project in southern Alberta, Canada. High-quality stacked reflection records are obtained from baseline and monitor DAS VSP surveys at the FRS and TL attenuation-attribute differences are derived from these reflection records. TL variations of attenuation attributes are observed within the injection zone at the FRS, which are interpreted as being related to the injected CO_2. Although there is always a significant trade-off between the accuracy and temporal resolution of the measured attenuation parameters, reliable attenuation measurements around the injection zone are still achieved with in-use reflection signal of a sufficient length and bandwidth. Attenuation attributes measured from this approach can be an advantageous tool for monitoring the distribution and migration of CO_2 plumes, especially for TL monitoring with DAS data that is with high noise level or with apparent acquisition or noise difference between different vintages.

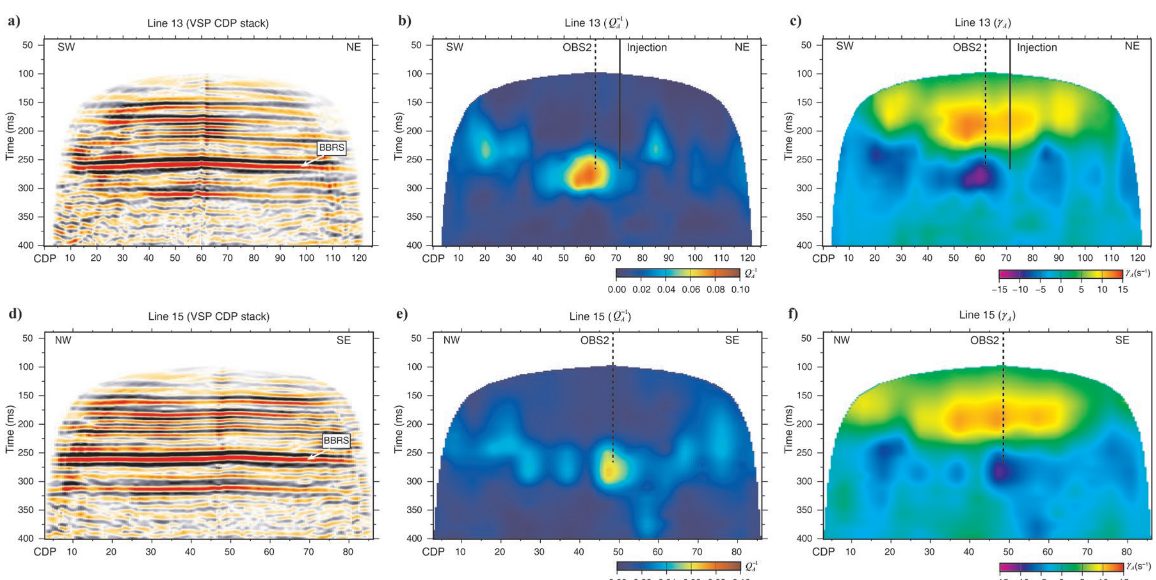

FIG. 6. Attenuation-attribute measurements from monitor data along (a-c) SW–NE Line 13 and (d-e) NW–SE Line 15: (a and d) monitor VSP CDP stack with BBRS reflection indicated, (b and e) estimated Q_A^{-1}, and (c and f) estimated γ_A. Dashed and solid black lines indicate OBS2 and injection well (labeled), respectively.

Back-projection imaging of physically-modelled seismic data

Joe Wong and Kevin W. Hall

ABSTRACT

FWI of measured wavefields yields high resolution images of velocity/density structures but can be very slow if the starting model is far from the true model. We recorded physically-modelled seismograms across a 2D region containing isolated targets, and demonstrate that back-projecting travel-time and amplitude anomalies is able to quickly create starting models close to the actual model in location, size, and shape.

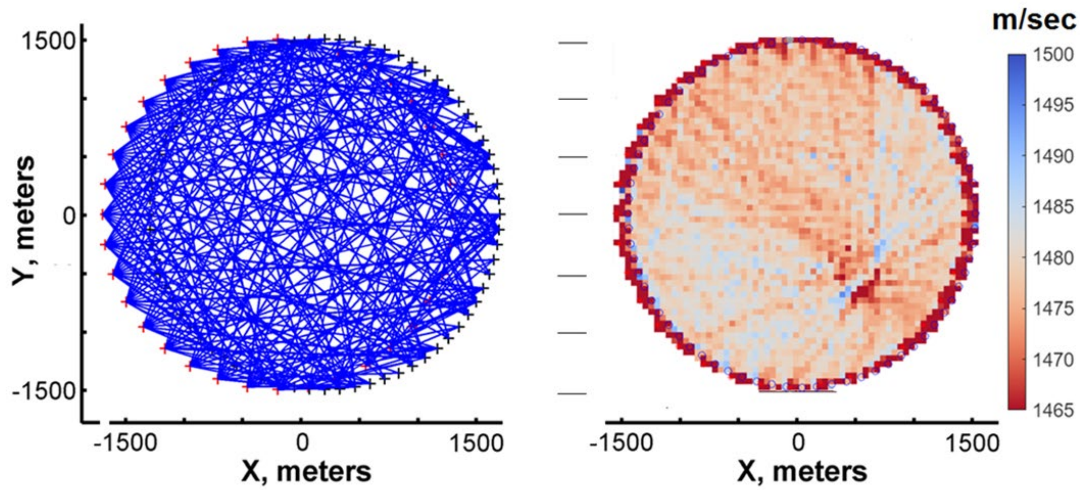

FIG. 1. Left: Scanning pattern for acquiring a set of transmission seismograms across a 2D plane in a physical modelling experiment. Right: Velocity image after 10 iterations of back-projecting first-arrival-time residuals. Though noisy, the image still indicates the presence of an isolated target.

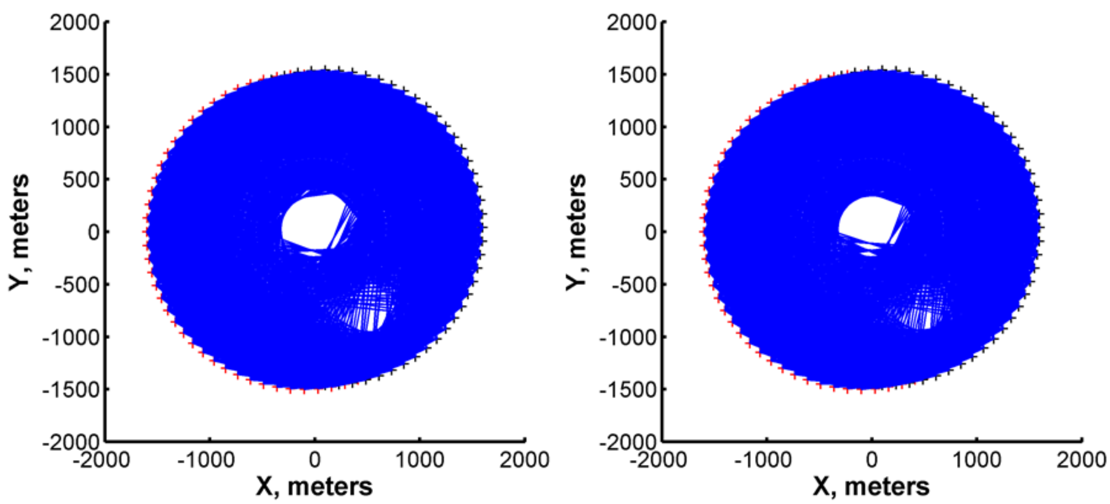

FIG. 2. Simple back-projection of rays from a time-lapse experiment produces clear evidence of two isolated targets. Rays are drawn or not depending on amplitude ratios on co-located traces from the baseline and monitor surveys, The two images are slightly different due to slightly different ratio values used for deciding whether or not to draw a ray.

Auto-adjoint elastic FWI: a time domain elastic full waveform inversion accelerated by CUDA with automatic adjoint-source calculation using various kinds of objective functions

Tianze Zhang*, Daniel Trad, Kris Innanen, and Jian Sun

ABSTRACT

We propose the Auto-adjoint time domain elastic full waveform inversion in this report, which is a FWI framework accelerated with CUDA using adjoint sources calculated with automatic differential method. In this FWI framework, the forward modeling and the adjoint modeling are accelerated by CUDA, and the adjoint sources are calculated by the automatic differential method. These two features allows us to perform time domain FWI with GPU acceleration and explore how different kinds of objective functions can influence the inversion results effectively. We study the objective function behavior for the $\ell 2$-norm. $\ell 1$-norm, Global-correlation based, Envelope based, objective function, and $\ell 1$-norm between the real and imaginary part of the synthetic data and the observed data ($\ell 1$-norm RI objective function). According to the numerical test we did in this paper, the $\ell 1$-norm RI objective function has better ability to tolerate the noise when poor initial model is used for inversion, compared with all the other objective functions we considered.

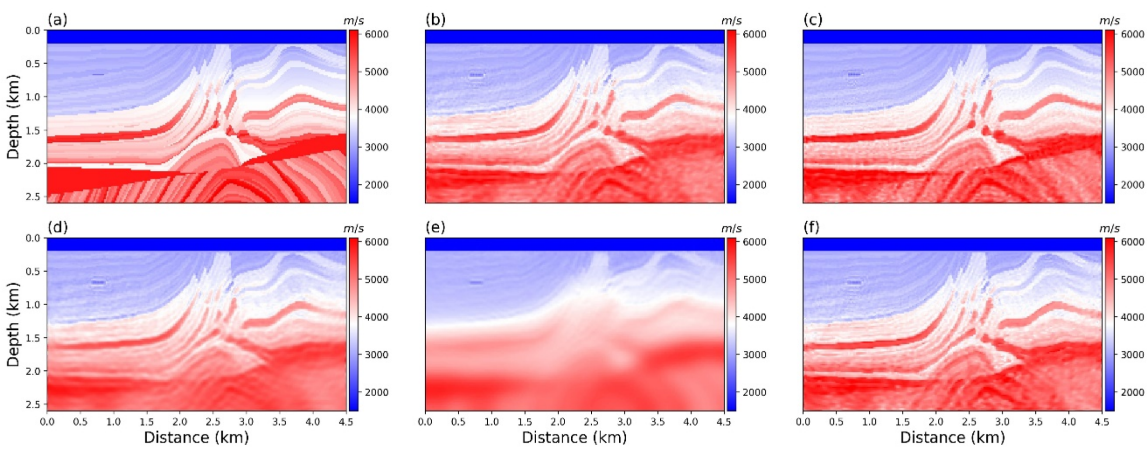

FIG. 1. Inversion results for Vp. (a) true Vp. (b) $\ell 2$-norm Vp inversion result. (c) $\ell 1$-norm Vp inversion result. (d) Envelope-based Vp inversion result. (e) Global-correlation-based Vp inversion result. (e) $\ell 1$-norm Vp inversion result.

Elastic full waveform inversion results uncertainty analysis: a comparison between the model uncertainty given by conventional FWI and machine learning methods

Tianze Zhang, Scott Keating, and Kris Innanen

ABSTRACT

Uncertainty analysis is an important aspect of quantifying the results of the inversion problem. In this report, we compare the uncertainty analysis given by two methods for full waveform inversion. The first method is by using the approximation of the inverse Hessian to perform the uncertainty analysis, as the approximation of the inverse Hessian is closely related to the posterior model covariance matrix. The second method is based on a machine learning-based method, which uses the Bayesian neural network (BNN) to generate elastic models and then performs the inversion. In the BNN, each trainable weight is represented as a Gaussian distributed probability distribution function (pdf). When BNN is well trained, we can forward calculate the BNN several times and perform the statistical analysis for the prediction results and give the uncertainty analysis for the generated models. Our numerical results suggested that both methods can generate promising inversion results and reasonable uncertainty quantification when compared with the true model errors.

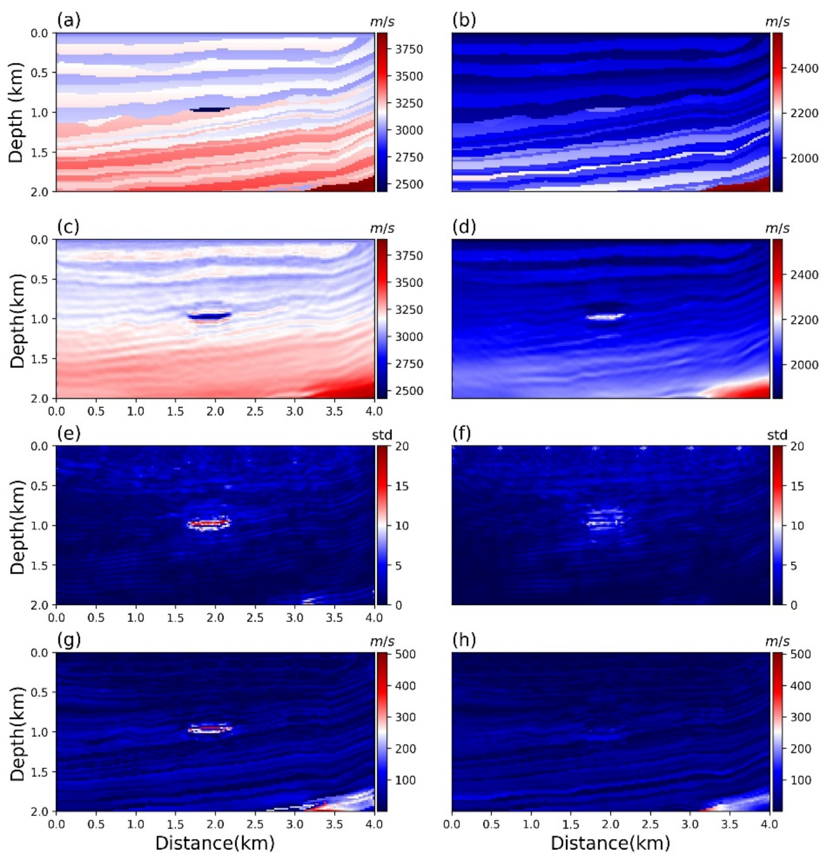

FIG. 1. FWI uncertainty analysis. (a) True Vp. (b) True Vs. (c) Vp inversion result. (d) Vs inversion result(e) Vp standard deviation. (f) Vs standard deviation. (e) Absolute Vp model error. (f) Absolute Vs model error.

Exact location DFT interpolation on GPUs and a look into processing kernels.

Kai Zhuang* and Daniel Trad

ABSTRACT

We look at the computation of the naive DFT interpolation on GPUs in an attempt to solve two main issues commonly seen in the application of 5D interpolation, compute times and far offset approximations. Our results show that the implementation on GPUs help solve both problems, although the computation of the naive DFT is significantly more expensive than the FFT, the switch to GPU computation for the dataflow decreases the runtime compared to standard CPU implementation of DFT interpolation. Generally, 5D interpolation is very compute intensive due to the sheer data volume sizes seen in today's seismic acquisitions size in multiple terabytes of data. As 5D interpolation must be performed on the entire dataset, it represents a significant amount of computational time spent on processing a dataset. Often, days of server time are spent interpolating data to improve sampling information and data uniformity. With our application of the 5D workflow into GPUs, we can attempt to significantly reduce the runtime due to the massively parallel nature of GPU processors. As a simple anecdote, GPU processing is more akin to parallel processing whereas CPU processing is more in line with 'multi-serial processing'. This computational advantage afforded to GPUs allows us to leverage some computationally more expensive operators to perform our interpolation at a higher accuracy. Mainly the Fourier transform algorithm that is used for standard 5D interpolation uses evenly sampled bins so that the data can be used in an FFT algorithm. This use of bins causes approximations in the 5D algorithm that can result in inaccuracies in the interpolated result. In our approach, we remove the binning part of the workflow in favor of using a more expensive naive DFT operator instead of the standard FFT operator.